FABRICATION AND CHARACTERIZATION OF DOUBLE-WALLED MICROSPHERE AS A DRUG DELIVERY SYSTEM FOR STROKE TREATMENT

Danni Zou

Thesis submitted to the University of Ottawa

in partial fulfillment of the requirements for the degree of

MASTER OF APPLIED SCIENCE

in Biomedical Engineering

Department of Chemical and Biological Engineering

Faculty of Engineering

University of Ottawa

Abstract

Stroke is a medical condition in which poor blood flow to the brain results in cell death. The current treatment options are limited and only very few patients can benefit from these treatments. Stroke causes brain swelling and often a decompressive craniectomy is performed for some of the patients to release intracranial pressure to prevent further damage. As a result, a duraplasty is implanted to replace the surgically-damaged dura mater to protect the brain. In view of that, the purpose of this project was to develop double-walled microspheres (DWMS) which can be used as a drug delivery system when incorporated into duraplasty to promote endogenous stem cell therapy to treat stroke. The DWMS were composed of poly (l-lactic acid) (PLLA) and poly (lactic-*co*-glycolic acid) (PLGA) using a solvent evaporation method. Bovine serum albumin (BSA), as a model protein, was entrapped within these DWMS with different core-shell thicknesses and compositions to investigate the distribution of protein, encapsulation efficiency, and *in vitro* release. The fabrication process parameters of DWMS were also optimized to attain higher yields, and the phase separation and surface morphology were examined by differential scanning calorimetry and scanning electron microscopy.

Keywords: Stroke; Duraplasty; Double-walled microspheres; Drug delivery; Burst Release

Résumé

L’accident vasculaire cérébral est une condition médicale durant laquelle une faible circulation sanguine vers le cerveau provoque la mort des cellules. Les options de traitement disponibles sont limitées et peu de patients peuvent en profiter. L’accident vasculaire cérébral provoque un gonflement du cerveau et souvent, certains patients subissent une craniectomie décompressive afin de libérer la pression intracrânienne pour empêcher plus d’endommagements. Par conséquent, afin de protéger le cerveau, une duraplastie est implantée pour remplacer la dure-mère chirurgicalement endommagée. L’objectif de ce projet alors était de développer des microsphères à double paroi qui peuvent être utilisées comme système d'administration de médicaments lorsqu'elles sont incorporées dans la duraplastie, afin de promouvoir la thérapie par cellules souches endogènes pour traiter les accidents vasculaires cérébraux. La microsphère à double paroi a été composé de poly (acide 1-lactique) (PLLA) et de poly (acide lactique-co-glycolique) (PLGA) en utilisant une méthode d'évaporation de solvant. L'albumine de sérum bovin (BSA), en tant que protéine modèle, a été piégée dans ces microsphères à double paroi avec différentes épaisseurs et compositions de noyau-enveloppe, pour étudier la distribution de la protéine, l'efficacité d'encapsulation et la libération *in vitro*. Les paramètres du processus de fabrication de la microsphère à double paroi ont également été optimisés pour atteindre des rendements plus élevés. De plus, la séparation de phase et la morphologie de surface ont été examinées par calorimétrie différentielle à balayage et microscopie électronique à balayage.

Mots clés: Accident vasculaire cérébral; Duraplastie; Microsphère à double paroi; Administration de médicaments; Libération par éclatement

Statement of originality

The content presented in this document is the product of original work performed by the author at the University of Ottawa under the supervision of Professor Xudong Cao.

In partial fulfillment of the requirements for the degree of Master of Science (Biomedical Engineering) at the University of Ottawa, this work was presented at the Ottawa Carleton Institute for Biomedical Engineering Seminar Series:

Danni Zou, Xudong Cao. *Fabrication and characterization of PLLA and PLGA double-walled microsphere as a drug delivery system for stroke treatment*. Ottawa Carleton Institute for Biomedical Engineering, April 2020.

A poster on the same topic was presented at the 70th annual Canadian Chemical Engineering Conference:

Danni Zou, Xudong Cao. *Fabrication and characterization of PLLA and PLGA double-walled microsphere as a drug delivery system for stroke treatment*. CSChE2020, October 2020.

Statement of contribution

The entirety of this document was written by the author. All figures and tables were created by the author unless otherwise mentioned in the caption. The work presented was largely performed by the author including fabrication and characterization of the microspheres. The cryo-sectioning of the double-walled microspheres was partially performed by Tongda Li.

Acknowledgements

First, I would like to thank my supervisor Dr. Xudong Cao for his consistent support throughout this journey. I am very grateful for the opportunities that he has provided and for his enthusiasm about the project.

Second, I would like to thank Dr. Chenfeng He for her guidance, patience and encouragements. I would also like to thank Hesham Ismail and Tongda Li for all of their help with this work as well as the other members of my lab for being so kind and providing moral support.

Third, I would like to thank my family and friends. Thank you for always encouraging and believing in me.

Table of Contents

List of Abbreviations

aFGF	acidic fibroblast growth factor
BBB	Blood brain barrier
BC	Biosynthesized cellulose
BCA	Bicinchoninic acid
BDNF	Brain-derived neurotrophic factor
bFGF	Basic fibroblast growth factor
BSA	Bovine serum albumin
CNS	Central nervous system
CsA	Cyclosporin A
CSF	Cerebrospinal fluid
DC	Decompressive craniectomy
DCM	Dichloromethane
DDS	Drug delivery system
DG	Dentate gyrus
DSC	Differential scanning calorimetry
DWMS	Double-walled microspheres
EA	Ethyl acetate
EVT	Endovascular thrombectomy
ECM	Extracellular matrix
EE	Encapsulation efficiency
EGF	Epidermal growth factor
FDA	US Food and Drug Administration
FGF	Fibroblast growth factor
FM	Fluorescent microscopy
GFs	Growth factors
HAMC	Hyaluronan and methylcellulose
HGF	Hepatocyte growth factor
ICH	Intracerebral hemorrhage
IV	Intravenous
MCAO	Middle cerebral artery occlusion
MSCs	Marrow stromal cells

NHS	N-hydroxysuccinimide
NGF	Nerve growth factor
NPC	Neural progenitor cells
NSCs	Neural stem cells
PACA	Poly (alkyl cyanoacrylates)
PBS	Phosphate buffer solution
PEA	Poly (ester amide)
PEG	Poly (ethylene glycol)
PHEMA	Poly (hydroxyethyl methacrylate)
PLGA	Poly (lactic-*co*-glycolic acid)
PLLA	Poly (l-lactic acid)
PVA	Poly (vinyl alcohol)
SEM	Scanning electron microscope
SGZ	Subgranular zone
SVZ	Subventricular zone
SWMS	Single-walled microspheres
TE	Tissue engineering
Tg	Glass transition temperatures
TIA	Transient ischemic attack
tPA	Tissue plasminogen activator
VEGF	Vascular endothelial growth factor

List of Figures

List of Tables

1. Introduction

Stroke is one of the leading causes of death and physical disability around the world[1-3]. Traditional treatment options such as oral administration, intravenous and intra-arterial injections of drugs are not sufficient since only a small portion of the therapeutic drugs can reach the brain because of the blood-brain barrier (BBB)[4-7]. Currently, tissue plasminogen activator (tPA) is the only U. S. Food and Drug Administration (FDA)-approved treatment option for ischemic stroke and has been shown to significantly improve survival outcomes and residual disability[8, 9]. Unfortunately, this treatment is known as a double-edged sword: it can only be used in the acute phase of stroke with a carefully measured drug dose and the therapeutic window is narrow (i.e., within 4.5h of stroke onset), leading to only 7% of stroke patients being eligible for this treatment[10-12]. In addition to tPA, the only other option available for ischemic stroke treatment is endovascular mechanical thrombectomy, promoting a more effective recanalization than thrombolysis. However, this treatment is still time-dependent as it can only be performed within the first 24h of stroke onset in selected patients [13]. Furthermore, it still needs to refine technical challenges as well as increase its accessibility to hospitals [14-16]. Up to now, there are no effective clinical treatments available for hemorrhagic stroke as few leads to improved functional recovery[17-20].

Stem cell therapy has been developed as a potential alternative to treat stroke[1, 21]. It is based on the regenerative capacity of certain parts of the adult brain. It is classified into two main categories: endogenous and exogenous approaches[21]. Due to the ethical and regulatory concerns and immune issues, limitations are imposed for exogenous stem cell therapy treatment for stroke[22, 23]. Endogenous stem cell approach is considered a better therapeutic option since it utilizes the stem cells already present within patients. However, the regeneration of newborn neurons by endogenous stem cells is insufficient to compensate for lost neurons in an injured brain due to insufficient trophic factors to stimulate their survival and

differentiation[24, 25]. To this end, growth factors (GFs) have been shown to promote stem cell differentiation, survival and trophic cell support in pre-clinical and clinical studies[26, 27]. In endogenous neurogenesis, GFs induced adult neural stem cells to proliferate and differentiate from the subventricular zone (SVZ) and the dentate gyrus (DG) into mature neurons and also to migrate to damaged brain tissue in both animal and human studies[28-31]. This implies that GFs could be an ideal therapeutic candidate to stimulate proliferation, differentiation and migration and enhance the survival of endogenous stem cells by modulating pathways of endogenous neurogenesis.

Decompressive craniectomy (DC) is a surgical procedure that is often performed on stroke patients to release intracranial pressure and relieve brain swelling caused from stroke[32, 33], and a duraplasty is commonly implanted to replace the surgically-damaged dura mater layer around the surface of the brain. Our lab has designed a drug-releasing duraplasty using biosynthesized cellulose (BC)[34]. However, the drug release only lasted for 10 days when we loaded the drug directly into the BC duraplasty. To achieve a more sustained release of growth factors to stimulate endogenous stem cells, double-walled microspheres (DWMS) composed of biodegradable polymers were used to encapsulate drugs or other active agents to prepare a drug delivery system to be incorporated into BC duraplasty. Microspheres have been used widely as drug carriers for tunable release[35-39]. In particular, DWMS with drug loaded in the inner core and engulfed by a drug-free outer shell, is more advantageous than single-walled microspheres (SWMS)[40]. Its initial burst release is lower than SWMS since the drug is encapsulated within the inner core rather than being located on the surface of microsphere[41, 42]. It can stabilize and protect the drugs with two layers and provide a prolonged period for up to several months[43].

The purpose of this thesis was to develop a drug delivery system that could perform a sustained release of growth factors to enhance endogenous stem cell proliferation, differentiation and migration for stroke treatment. Therefore, the objectives of the thesis are:

1. To prepare DWMS using poly (l-lactic acid) (PLLA) and poly (lactic-*co*-glycolic acid) (PLGA) and to optimize the fabrication procedure.
2. To characterize the properties of the DWMS, including morphology, size analysis, core-shell layer analysis, thermal analysis, drug encapsulation efficiency, drug loading localization, and drug release profile will also be characterized. In this thesis, bovine serum albumin (BSA) is used as a model drug.

2. Literature Review

2.1 Stroke

Stroke, also known as cerebrovascular accident, is the second leading cause of death and the third leading cause of disability worldwide[3, 21, 44]. According to the World Health Organization, 15 million people suffer from strokes worldwide each year[45]. In Canada, stroke is the third killer of adults, and the primary cause of physical disabilities and mental disabilities[46]. More than 62,000 strokes occur in Canada each year[47]. Stroke is characterized by sudden death of some brain cells due to lack of oxygen and nutrients when the blood flow is inhibited by blockage or rupture of an artery to the brain. There are three main types of stroke: ischemic stroke, hemorrhagic stroke, and transient ischemic attack (TIA). Ischemic stroke is the most common form of stroke, accounting for 87% of all strokes. It happens when blood clots block the blood flow through the artery that supplies oxygen-rich blood to brain[48, 49]. Hemorrhagic stroke occurs when an artery in the brain leaks blood or ruptures, causing high pressure resulting in brain cell damage[50, 51]. It only accounts for 13% of all strokes but contributes to about 40% of all stroke deaths. Transient ischemic attack, also

known as a mini-stroke, occurs when an artery is briefly blocked by a small clot that stops blood flow for no more than 5 minutes usually[52, 53]; TIAs are often considered as a significant warning sign of a more serious stroke that might occur.

2.1.1 Approaches to overcome stroke

Currently available stroke treatment options are very limited. Emergency treatment for stroke varies depending on which type of stroke a patient has.

2.1.1.1 Treatments for ischemic stroke

For ischemic stroke and TIA, these strokes are caused by blood clots or other blockages in the brain. They are mainly treated with similar techniques that are discussed below:

Therapy with thrombolytic drugs breaks up blood clots in brain's arteries. An intravenous (IV) injection of tPA, also known as Alteplase IV r-tPA, is a gold standard treatment for acute ischemic stroke[12, 54]. It works by injecting tPA intravenously into the cerebral vessels, thereby dissolving the blood clot and restoring blood flow after stroke symptoms started[55, 56]. A lot of studies have shown the effectiveness of this treatment when performed during a narrow therapeutic window[57-60]. However, because the therapeutic window is within the first 3 to 4.5 hours of stroke onset[10, 61], only a small portion of stroke patients can benefit from this treatment. Moreover, there are some reported issues of tPA in clinical use. For example, since intravenous tPA has a short half-life of about 5 to 10 minutes, and acts on the clot surface only and barely dissolves old or large blood clots, merely 10-25% of stroke cases can accomplish effective and permanent recanalization of the occluded blood vessel[58, 62]. In addition, it has been shown that exogenous tPA can pass through both the intact and damaged blood-brain barrier (BBB) into ischemic brain tissue and exert neurotoxic effects[63-65]; in some cases, intravenous tPA has been documented to have caused fatal intracerebral hemorrhage (ICH)[66, 67].

Alternatively, endovascular thrombectomy has been confirmed to significantly improve outcomes and decrease long-term disability after acute ischemic stroke[68, 69]. The insertion of a catheter (thin tubes visible under X-rays) in the groin or the arm can remove a blood clot from an artery in the brain by encasing it in a stent which is then pulled out with the clot, or by sucking the clot through the catheter[70]. This treatment has a longer therapeutic time window than tPA injection alone but is still limited as it can only be applied to selected patients with acute ischemic after symptom onset within 6 to 24 hours[71, 72]. Stent-Retriever thrombectomy is often performed with injected tPA to directly remove the clot from the blocked vessel in the brain[11, 73]. It is beneficial for stroke patients who have large clots that cannot be dissolved with tPA completely, but the safety and long-term functional outcome of this procedure in patients who do not meet standard inclusion criteria for endovascular stroke treatment are unknown[74, 75]. Furthermore, only a few specialized stroke centers have adequate equipment and resources to provide this treatment[76].

2.1.1.2 Treatments for hemorrhagic stroke

When a hemorrhagic stroke occurs in the brain, the pressure within the skull increases. Therefore, the emergency treatments for hemorrhagic stroke involves measuring and lowering pressure. Medicines to lower intracranial pressure, decrease swelling and reduce pain may be administered. Moreover, in some cases, neurosurgical procedures or interventional radiology, such as coil embolization or surgical clipping, may be performed to repair the ruptured blood vessel and relieve the pressure caused by the bleeding and brain swelling[77, 78]. Surgical removal of the hematoma as an early-stage treatment for hemorrhagic stroke may improve long-term prognosis[79]. Unfortunately, there are currently no validated and targeted therapies that have been proven to stop the bleeding and enhance functional recovery after a hemorrhagic stroke occurs[80]. Prevention of high blood pressure from close monitoring in high-risk groups

is the best treatment for hemorrhagic stroke[81]. Hence, the development of effective treatments for hemorrhagic stroke is urgently needed.

2.1.1.3 Stem cell therapy

Stem cell therapy is an emerging therapeutic option for stroke treatment. Nearly four decades of preclinical studies have demonstrated the efficacy and safety of stem cells in stroke animal models[82]. Stem cells are immature cells with self-renewal capacity and differentiation ability to become different cell types for the life span of each individual[83, 84]. Stem cells are divided into different types based on where they originated: embryonic, fetal and adult stem cells. Embryonic stem cells derived from the blastocyst, are totipotent and contribute to progenies of the embryonic germ layers[85, 86]. Fetal stem cells are progenitor cells harvested from fetal blood, bone marrow as well as from fetal organs still undergoing major developmental changes[86, 87]. In spite of the fact that embryonic or fetal stem cells have potential benefits in the treatment of stroke[88-90], the use of these stem cells is limited since they raise sharp political and ethical controversies[21, 91]. Stem cells derived from the adult central nervous system (CNS) or bone marrow are promising alternative sources in stem cell therapies for stroke. This treatment aims to replace lost glial cells such as astroglia and oligodendroglia from infarcted tissue to re-maintain a functional neuronal circuitry and rebuild nerve conduction[92-94]. Furthermore, adult stem cell therapy targets the subacute and chronic phases of stroke, thereby significantly prolonging the effective time of intervention; many patients are likely to benefit from this treatment[94, 95]. Stem cell therapy for stroke is classified into two types: exogeneous and endogenous stem cell therapy[96, 97] as shown in Figure 1.

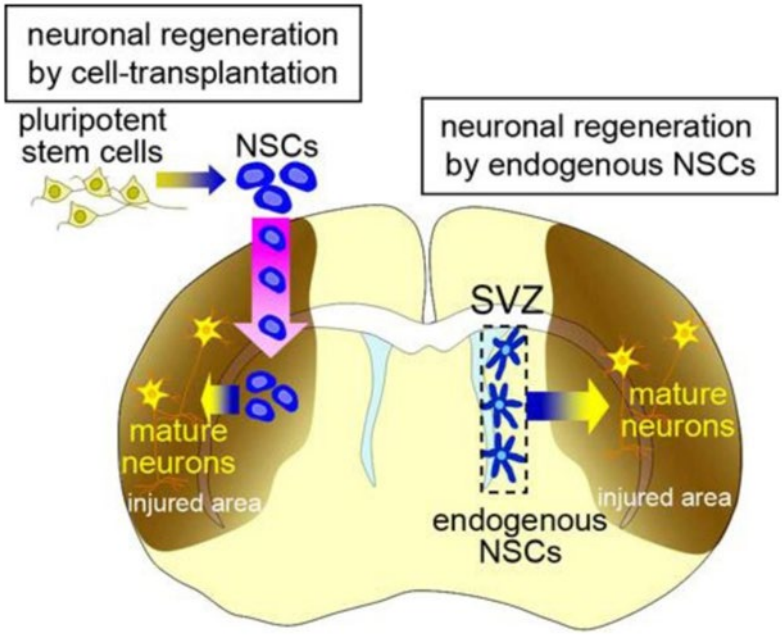

Figure 1. Schematic showing exogenous (left) and endogenous (right) stem cell therapy for stroke treatment using neural stem cells (NSCs)[98].

The exogenous approach involves transplantation of stem cells delivered locally (e.g., intracerebral) or systemically (e.g., intravenous or intraarterial) and *in vitro* culture of cells prior to purification and administration[21, 99]. Recent research of exogenous stem cell therapy for stroke has demonstrated promise. Chen *et al.* found when allogenic bone marrow stromal cells (MSCs) were intracerebrally transplanted into the ischemic boundary zone of a middle cerebral artery occlusion (MCAO) adult rat model, MSCs could survive, differentiate into phenotypic neural cells and enhance functional recovery from stroke[100]. Zhang *et al.* isolated and transplanted adult neural stem cells (NSCs) derived from the SVZ of young adult rats into ischemic rats. Their results showed those transplanted NSCs could survive, migrate towards the lesion, differentiate into neurons and significantly improve neurological function[101]. Taguchi *et al.* reported induced perilesional angiogenesis and subsequent neurogenesis occurred in mice after 48 hours post-stroke, as a result of systemically administrated human cord blood-derived-CD34+ cells[102]. Shyu *et al.* also confirmed that intracerebrally implanted peripheral blood stem cells resulted in neurogenesis and angiogenesis along with transplanted cells differentiating into neurons, vascular endothelial cells and glial cells in rats

after chronic cerebral ischemia, thus amplifying neuroplastic effects in the ischemic brain[103]. The study of the application of heterogenetic MSCs was investigated by Bao *et al.* They injected human MSCs in rat ipsilateral brain parenchyma one day after intracerebral hemorrhage. The results demonstrated the transplantation of MSCs significantly decreased inflammatory infiltration and heightened angiogenesis, along with the depletion in brain edema and significant recovery of behavior[104]. The major challenges of exogeneous stem cell therapy include the acquisition of adequate stem cells since some stem cells such as the organ-originated stem cells are hard to collect due to their unique location and limited quantity[105]. Poorly controlled experimental condition for the *in vitro* culture leads to their genetic instability, chromosomal aberrations and loss of differentiation capacity[106]. In addition, exogenous stem cell transplantation may give rise to tumorigenesis[107]. Moreover, stem cell transplantation requires surgical intervention in some cases, which is highly invasive.

The endogenous approach aims to stimulate mobilization of stem cells present within the individuals to amplify neurogenesis[21]. Mobilization of host stem cells is easier than exogenous transplantation because it avoids the complication of transplantation of stem cells including surgical trauma, graft rejection and tumor formation. In humans and animals, endogenous NSCs are present in two regions, the subventricular zone (SVZ) of the lateral ventricles and the subgranular zone (SGZ) of the dentate gyrus (DG)[86]. It has been shown that in preclinical stroke models, transplantation of NSCs not only enhanced the proliferation of endogenous NSCs in the SVZ and DG, but also promoted the migration of endogenous neuroblasts to the brain lesion region which differentiated to mature neurons, thereby augmenting endogenous neurogenesis to replace lost neuronal cells[8, 18, 108]. This was achieved by growth factors (GFs) stimulation of NSCs proliferation, differentiation, migration and trophic cell support[109, 110]. Several different growth factors are currently being studied including: brain-derived neurotrophic factor (BDNF)[111, 112], vascular endothelial growth

factor (VEGF)[113, 114], nerve growth factor (NGF)[115, 116], epidermal growth factor (EGF)[117, 118], and fibroblast growth factor (FGF)[117, 119-121].

The use of growth factors as a direct therapeutic agent for stroke treatment has been under investigation in rodent models. For example, intranasal acidic fibroblast growth factor (aFGF) treatment has been indicated to promote angiogenesis in the boundary regions of brain ischemia, enhance the proliferation of neural progenitor cells from SVZ, and induce newly born neuroblast to migrate from the SVZ to the ischemic lesions at day 14 after MCAO[121]. Sugimori *et al.* demonstrated continuous intravenous infusion of basic fibroblast growth factor (bFGF), that was performed for three hours after the onset of ischemia, could persistently decrease infarct volume by 27% for at least three months in focal cerebral ischemia adult rat models compared with control groups[122]. Ninomiya *et al.*[123] and Teramoto *et al.*[118] reported intraventricular administration of EGF enhanced the proliferation of doublecortin positive neuroblasts in the SVZ as well as the neuroblast migration out of the SVZ to the ischemic lesion and the differentiation into mature neurons. VEGF, effectively stimulating formation of new blood vessels and vascular permeability, positively affected acute and chronic stroke[124]. A three-day intracerebroventricular infusion of VEGF after temporary MCAO in rat models reduced infarct volume, enhanced survival of newborn neurons in SVZ and DG and angiogenesis in the infarct penumbra[125]. It has been stated that intranasal administration of NGF decreased infarct volumes and improved neurological outcome after seven days MCAO in rat models. In addition, NGF treatment improved angiogenesis in the peri-infarct region, promoting neurological functional recovery after ischemic stroke[126]. In rat MCAO models of ischemia, pre-treatment with intraventricular or intravenous BDNF dramatically decreased the infarct volume and neuronal cell death. It also promoted neurogenesis in DG and induced migration of SVZ progenitor cells to the nearby striatum of the ischemic hemisphere[127, 128]. Furthermore, the synergisms between growth factors has been shown to enhance nerve

regeneration[129]. For example, the application of both EGF and bFGF has been demonstrated to promote the long-term survival and proliferation of neural stem/progenitor cells[34, 130]. The VEGF and bFGF have synergistic effects on the induction of angiogenesis[131, 132].

Although the use of growth factors is a promising avenue for treating stroke, more studies are necessary to perform optimal dosing, timing and methods of administration, as well as possible combination of growth factors and their effects and further pre-clinical testing. Growth factors generally are large polypeptides, some of which do not significantly cross the BBB[133, 134]. Many studies have used invasive administration to inject or implant growth factors directly into brain tissue (e.g., intraparenchymal, intracerebroventricular, intrathecal, intracisternal administration) to bypass BBB[135-137]. Conversely, current data suggests that there are growth factors such as hepatocyte growth factor (HGF) which could cross the intact BBB via facilitated transport systems[138, 139]. Furthermore, focal stroke causes BBB disruption, permitting passage of both large proteins and cells. In view of that, several studies have applied systemic administration of growth factors (e.g., intravenous, intraperitoneal, subcutaneous administration)[140]. Additionally, even though the exogenous growth factors trigger NSCs proliferation, promote NSCs to migrate towards the stroke site and differentiate into neurons, these NSCs were often observed far from the stroke cavity or the peri-infarct area[141]. This could be overcome by using biomaterials such as hydrogels loaded with growth factors to impact the migration of endogenous NSCs from the SVZ into the stroke cavity[8, 142, 143].

2.1.2 Decompressive Craniectomy (DC)

While the therapeutic treatments for stroke are limited, there are still options for treating the symptoms and preventing further severe damage. Brain swelling, as known as cerebral edema, is an urgent clinical condition that accompanies some cases of stroke[144, 145]. It is caused by damaged brain cells due to stroke trapping the drainage of cerebrospinal fluid (CSF)

from the brain[144]. The fluid increases the intracranial pressure, which slows brain blood flow and reduces oxygen level in the brain. A decompressive craniectomy (DC) is usually performed after a brain swelling. Through DC, a significant portion of the skull is surgically removed, which allows the swollen brain to herniate outward rather than compress normal structures. This prevents the brain from brain stem herniation and secondary damage due to elevated intracranial pressure, and has also been shown to be life-saving[33, 146-148]. Although DC is an invasive last resort procedure and does not improve functional or neurological recovery outcomes, it substantially lowers the risk of mortality in patients[149-151].

2.2 Protective layers of the brain

During a DC, a surgeon will remove a part of the skull and cut the dura mater to allow the pressure to release. The brain is surrounded by three outer protective layers called meninges under the skull. The meninges layered in order from the outermost inward are dura mater, arachnoid mater, and pia mater[152]. Their positioning around the brain can be seen in Figure 2. The meninges help to keep the CNS in place to prevent the brain from moving within the skull[153]. The outermost layer, the dura mater, is a tough, thick and dense membrane. It keeps the CNS fastened to the skull and supports the dura venous sinuses to carry blood from the brain to the heart[154]. As a connection of the dura and the pia mater, the arachnoid is an extra barrier to isolate CNS from the body to keep fluids and toxins out of the brain[155]. The arachnoid is also the place filled with CSF which acts as a cushion to allow the brain to suspend and preserve the brain's shape[156]. The pia mater, which is another thin membrane, helps to obstruct fluids and aid the CSF production[154].

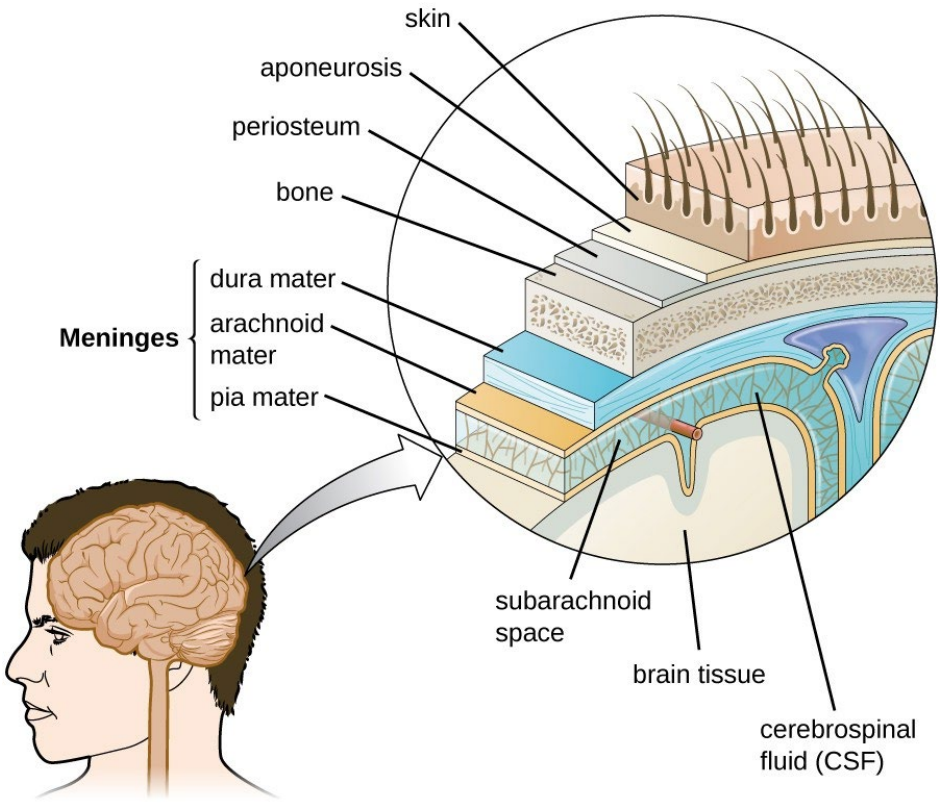

Figure 2. The layers of tissue surrounding the human brain contain three meningeal membranes: the dura mater, arachnoid mater, and pia mater[157].

2.3 Duraplasty

A duraplasty is a surgical reconstruction of the dura mater after DC, in which the cut dura mater was replaced by another biocompatible soft material. There are a variety of materials which have been used experimentally and clinically for dura mater grafting, from metal sheets and autologous body tissues to allogeneic tissues, xenogeneic tissues and biosynthetic materials [158-161]. Autografts, such as galea[162] and fascia lata[158, 163], are grafts that have been harvested from the same individual. They are easy to handle, nontoxic, inexpensive, and do not provoke inflammatory or immunological reactions[164]. However, autograft is not possible when used to close large dural defects[165, 166]. The application of autologous grafts from other areas of the body needs an additional surgical operation, which increases operation time and patient morbidity. Allografts are grafts between genetically different individuals of the same species. Allogeneic dura maters, such as cadaverous dura mater allografts[167] and amniotic membrane[168], have been used but there is a lack of

allogenic donors and allografts are not completely free from the risk of transmission of latent virus and prion infections[169, 170]. Xenografts are grafts originated from a different species. Xenografts such as bovine pericardium[171], porcine dermis[172, 173] and processed collagen matrices[174, 175] have been employed for dural reconstitution. However, the major shortcomings of these grafts are the increased risk of immune reactions and infection, scarring, graft dissolution and adhesion formation[161, 176, 177]. Some synthetic materials such as silatic and expanded poly(tetrafluoroethylene) (ePTFE) were used as duraplasty but they can lead to undesirable tissue reaction, excessive scar formation, meningitic symptoms or hemorrhage risk[178, 179]. Natural biomaterials such as alginate[180, 181] or cellulose[182, 183] have shown promising results as dural graft substitutes. These materials are capable of restoring the dural defect and create optimal conditions for the development of connective tissue at the site of injury.

An ideal duraplasty material should meet all the following criteria. First, it should be biocompatible with non-toxicity and immunological inertness[158, 184, 185]. Second, it should have sterility to prevent the spread of virus and parasite[186, 187]. Third, it should have reasonably high mechanical properties to withstand the operation of surgery as well as protect the brain while still maintaining its flexibility and elasticity[169, 188]. Fourth, it should be inexpensive and readily available to stock when needed[158].

2.4 Hydrogels

Hydrogel is a three-dimensional, hydrophilic cross-linked polymeric network, which is capable of absorbing large amounts of water or biological fluids while maintaining their strong mechanical and biocompatible properties[189]. Hydrogels are divided into biopolymer-based and synthetic-based according to their origins. A variety of natural polymers and their salts such as gelatin[190], collagen[191], sodium alginate[192], cellulose[193], and their derivatives[194] as well as synthetic polymers such as poly(ethylene glycol) (PEG) [195],

poly(vinyl alcohol) (PVA) [196] and poly(hydroxyethyl methacrylate) (PHEMA) [197] have been used to fabricate hydrogels. Numerous hydrogels have been widely explored in tissue engineering applications[198-201] and have been shown to be potential candidate materials in duraplasty applications[185, 202, 203].

2.4.1 Post-stroke treatment using hydrogels

Since hydrogels can be injected as liquids then solidified *in situ* or implanted gelatinous solids through surgeries as well as maintain similar mechanical properties to the brain, many researches have demonstrated the potentials of hydrogels for the treatment of stroke. Table 1 describes several hydrogels that are in use for stroke treatment.

Table 1. Summary of hydrogels used for treatment of stroke

Hydrogel Format	Therapeutic substance	Administration	Therapeutic effects	References
Microporous annealing particle-hyaluronic acid-based hydrogels	Hyaluronic acid hydrogel (porous)	Intracerebral administration to the stroke cavity of permanent MCAO mouse model at 5 days post-stroke	Decrease of astrogliosis and inflammation, promoted neurogenesis and angiogenesis, significant migration of neural progenitor cells to lesions	[142]
Cross-linked hyaluronan, heparin sulfate and collagen hydrogel	Neural progenitor cells (NPCs)	NPCs with hydrogel matrix transplanted into the stroke cavity 7 days after focal ischemia in mice	Reduction of inflammatory infiltration and cell stress, promoted survival of NPCs	[204]
Hyaluronic acid hydrogel	BDNF	Injection into the infarct core after 7 days in striatal stroke adult mice	Sustained release of BDNF for over 3 weeks, improved motor function recovery, increased the migration of immature neurons into the peri-infarct	[205]

			cortex and long-term survival	
Silk fibroin hydrogel	Silk fibroin hydrogel	Intracerebral injection into lesion cavity of adult male rats after 2 weeks of transient MCAO	Great space conformity to fill the stroke cavity, support endogenous cell proliferation, no overt inflammatory response and adverse morbidity	[206]
Hyaluronan/methyl cellulose (HAMC) hydrogel	Erythropoietin (EPO)	Epi-cortically injection at day 4 and day 11 post-stroke in mice	Reduced the size of stroke cavity and inflammatory response, improved the survival of neurons in the peri-infarct region and neuroblasts migration in the SVZ, and reduced apoptosis in the SVZ and the injured cortex	[207]
Thiolated gelatin hydrogel	Gelatin hydrogel	Injection into the lesion site of adult mice at 3 days post-	Reduced neuron loss, diminished neurological deficit	[208]

		intracerebral hemorrhage	post-operation, suppressed inflammation and enhanced functional recovery	
Hyaluronic acid-based hydrogel	Nogo-66 receptor antibody	Insertion of the hydrogel grafted with antibody into the ischemia region of adult rat model 2 weeks after MCAO	Improved behavioral recovery, neural migration and regeneration in the brain lesion	[209]

2.4.2 Cellulose

Among the natural polymers, cellulose is one of the most abundant natural polysaccharides on earth. It contains multiple hydroxyl groups, thus having great potential for hydrogel preparation. It is present in cell walls of plants (e.g., cotton, linen) and some bacteria as well (e.g., *Acetobacter xylinum*) [210]. It is a long chain of glucose units attached together by β-1,4-glycosidic linkages represented in Figure 3. The chains are arranged to form microfibrils through hydrogen bonding, which enables cellulose to have fascinating mechanical properties and chemical stability[210].

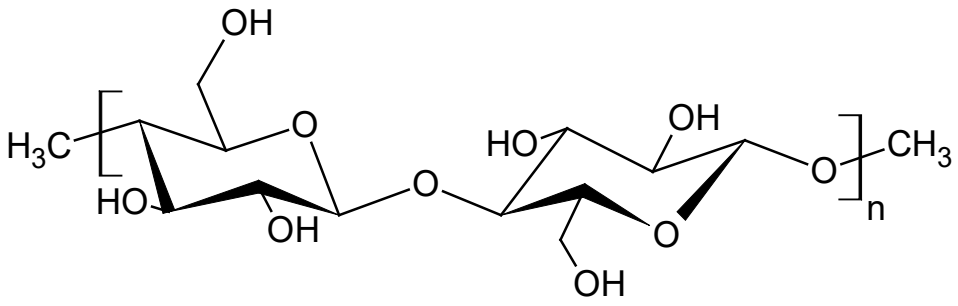

Figure 3. Chemical structure of cellulose[211, 212].

Plants and bacteria are both capable of synthesizing cellulose. Plants produce cellulose to make up their cell walls, while some types of bacteria produce cellulose around the cells to protect themselves from ultraviolet radiation, harsh chemical environments and access to oxygen[213, 214]. Bacterial cellulose, also known as biosynthesized cellulose (BC), has the advantage of higher purity compared with plant-based cellulose which needs to be separated from lignin and hemicellulose[215]. Also, BC has excellent water retention property and hydrophilicity[216]. It has been exhibited to hold up to 100 times more than the cellulose sample weight in water, whereas plant cellulose has only been shown to retain 60% of its weight[217-219]. In addition, BC can be produced on various substrates, and due to its high moldability during the formation, it can grow into almost any shape[219, 220]. Furthermore, compared with plant cellulose, BC has higher crystallinity and forms significantly smaller

microfibrils[221, 222]. These ultrafine microfibrils make BC more porous, which allows the BC to find many applications in biomedical fields. For example, BC and BC-based hydrogels are commonly used for applications in drug delivery[223-225], regenerative medicine[225-227], wound dressings[228, 229]. In addition, BC has been grafted as dura substitutes to replace and repair dura mater after intradural cranial surgery in animal models[230-232]. The results exhibit that BC has suitable biocompatibility with neither immune reactions and inflammatory response nor neurotoxicity. Our group has already successfully designed BC from *Gluconoacetobacter hansenii (G. hansenii)* as a drug releasing duraplasty[34]. Future steps of this thesis will further work on incorporating microspheres into BC to improve the drug delivery profile.

2.5 Drug delivery system

2.5.1 Overview of drug delivery system

Drug delivery systems (DDS) is defined as a formulation of a device that enables transport a drug or active agent to release in a predesigned way at a particular site. The conventional drug delivery systems, typically tablets or intravenous injection, feature immediate and uncontrolled drug release kinetics[233]. Both administer the entire dose of drug in one portion, which could contribute to too high drug concentration which is close to toxic threshold causing adverse reactions or too low drug concentration which is below effective therapeutic level to provide therapeutic benefits[233, 234]. This is of significant concern when a bioactive drug is applied with narrow therapeutic windows. Moreover, conventional delivery is unpredictable and inefficient. It requires repetitive drug administration, which is not only inconvenient to perform on patients but also could cause ineffective treatments since the drug levels in patients are fluctuated rapidly and do not keep long-term proper levels[235].

Controlled drug delivery systems have been developed to solve those problems. The controlled drug delivery system could release the drug in a well-controlled manner to maintain

the drug levels within the expected range for a long term[236]. In addition, it requires fewer administrations and increases the compliance of the patient[237]. Although there are significant advantages, the potential disadvantages of controlled drug delivery systems should not be neglected: the non-biocompatibility of the vehicle materials, undesirable degradation by-products, necessary surgery for implantation or removal of the system, and the higher cost of release systems than traditional pharmaceutical formulations[238-240].

2.5.2 Polymeric drug release systems

In the past decades, different biomaterials, such as metals, ceramics, alloys and polymers have been explored for controlling drug release[241, 242]. Among which, a large number of drug delivery systems have shown great developments to achieve extended drug release by taking advantage of polymers[243]. Polymers are large molecules formed by linking a series of simple repeating units. Various polymers have been applied to make matrix, reservoir and other implant forms because of the innate characteristics of polymers[243, 244].

Polymeric biomaterials have several advantages. The advantages include excellent physical, chemical, toxicological, mechanical and biological properties for extensive biomedical applications: transplants, medicine, cell therapy, orthopedics, biological adhesion, dental materials, surface functionalization, controlled delivery of therapeutics, tissue regeneration[198, 245-249]. Moreover, they have reasonable costs and easy accessibility compared to other biomaterials such as metal and ceramics[241]. In particular, polymeric biomaterials to be chosen successfully as drug delivery systems are biodegradable and biocompatible, chemically inert and free of leachable impurities[250, 251]. This means they are fragmented into biocompatible molecules which are metabolized and excreted from the host body through normal metabolic pathways as well as not trigger any adverse effect on the host[249, 252].

By using polymers as carriers, the drugs are incorporated within a polymer and can be released effectively by different mechanisms. The mechanisms of polymeric drug release systems can be controlled physically or chemically as shown in Figure 4. The physically controlled release mechanisms can be classified into diffusion-controlled and solvent-controlled systems[253]. Diffusion-controlled systems can be divided into reservoir type and matrix type. In a reservoir system, a drug is dispersed or dissolved in a core surrounded by a water insoluble polymeric membrane[254, 255]. The diffusion of drug is driven by the rate-controlling porous polymeric membrane, enabling the drug to migrate from the polymer to the environment. The drug release rate is affected by several factors including initial drug concentration, drug solubility, drug particle size, polymer composition, polymer degradation, the thickness of the coating.[256, 257]. A matrix-type system is when drug particles are homogenously dispersed within the insoluble polymer matrix[258, 259]. In a matrix-type system, it usually shows a high initial burst release since there is no membrane acting as a diffusion barrier, prior to a declining release rate accompanied by an increasing diffusion distance for drugs located at the interior of the carrier[258]. The solvent-controlled release includes osmosis-controlled and swelling-controlled release systems. Osmosis-controlled system consist of a drug core surrounded by a semipermeable polymeric membrane coated with one orifice[260, 261]. The semipermeable membrane is permeable to water but not to the drug. The water diffusion through the semipermeable membrane is driven by osmotic pressure, from the membrane exterior (low concentration of drug) to the drug-loaded core (high concentration of drug), until the solute concentrations are equal on both sides of the membrane[260, 262]. The drug solutes are then continuously diffused out of the membrane through the small delivery orifice over a prolonged period of time[260]. This type of release system consistently dispenses drug solutes at a zero-order rate given that a gradient is maintained consistently throughout the membrane[263, 264]. Swelling controlled release systems are initially dry and then uptake

water or other body fluids when placed in the body and swell[258]. Swelling increases the content of aqueous solvent within the formulation as well as the size of polymer mesh, allowing the drug to diffuse through the swollen crosslinked network into the exterior[265, 266]. The swelling-controlled system might achieve a zero-order drug release, depending on the polymer composition and initial drug distribution in the system[267, 268]. The chemically-controlled release mechanisms include degradation-controlled and polymer-drug conjugate-controlled systems[243, 269]. In degradation-controlled systems, drugs are encapsulated in biodegradable polymers by dispersion and released by polymer degradation and drug diffusion[270]. These polymers such as polysaccharides, polyesters and polyamides can be degraded through enzymatic and/or hydrolytic degradation. Polymers like PLGA, polylactic acid (PLA) undergo bulk degradation, which simultaneously degrades the entire matrix[258]. In contrast, polymers such as polyanhydrides and polyorthoesters typically degrade from the surface into the core (surface degradation) because the polymer degrades faster than water diffuses into the matrix[270, 271]. Drug release kinetics are controlled by the degradation rate of polymers, which depends on the end groups, molecular weight, monomer composition, and crystallinity[272]. In polymer-drug conjugate systems, drugs are attached covalently to the functional groups of polymers directly or via a spacer[273]. Enzymatic and/or hydrolysis degradation cleaved the drug and polymer covalent linkages to release and activate the drug. The drug release kinetics are controlled by the cleavage rate[243, 274]. Overall, the drug release rates are based on a series of parameters including polymer properties, drug properties, matrix geometry, initial drug loading, the interaction of drug and matrix.[243, 275-278]. Further studies have been examining how to optimize these parameters to attain the desirable drug release from polymeric drug systems.

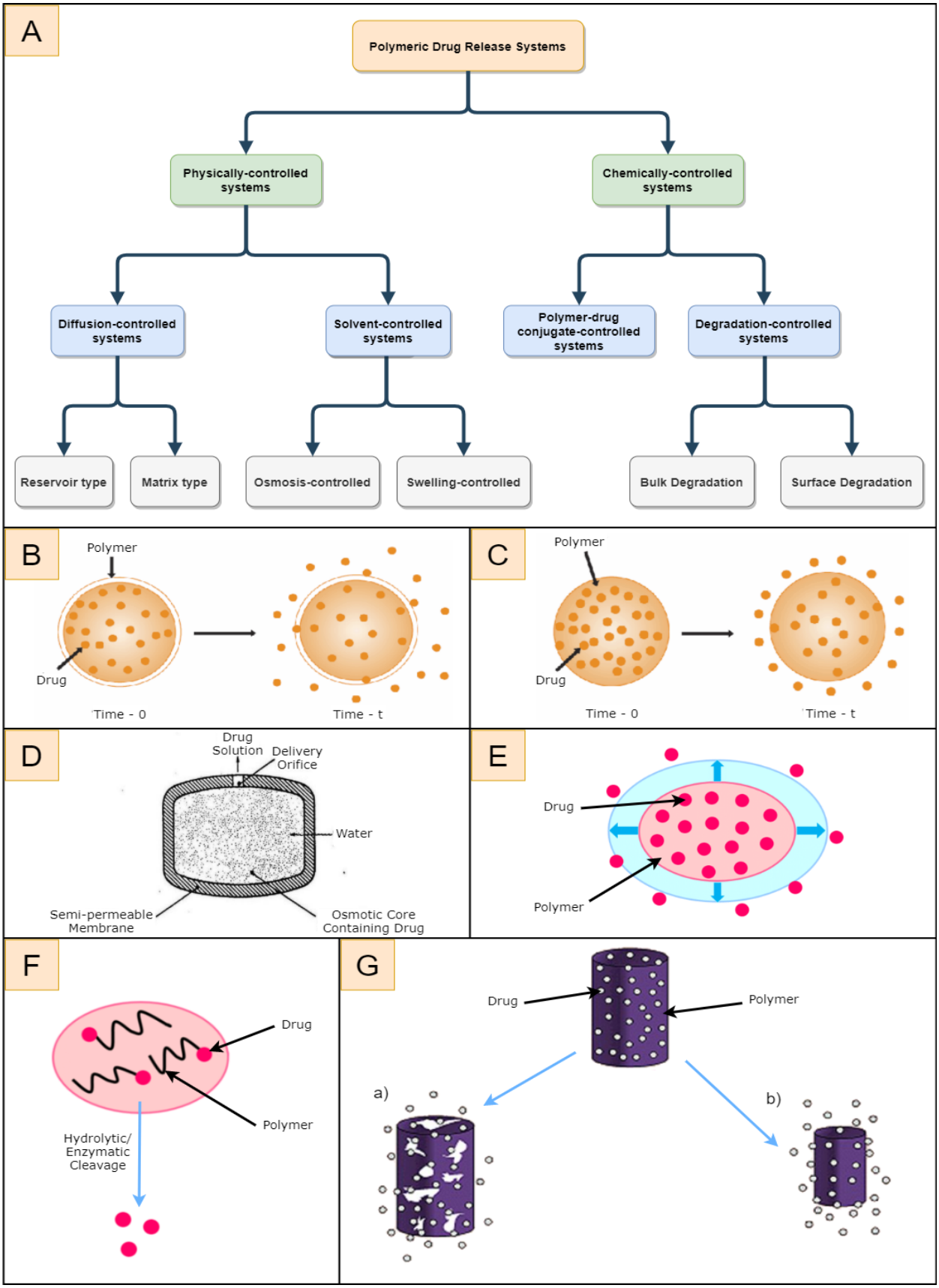

Figure 4. (A) Polymeric drug release systems. (B) Reservoir diffusion controlled drug delivery device[264]. (C) Matrix diffusion controlled drug delivery device[264]. (D) Osmotically controlled release system[264]. (E) Swelling controlled release system[279]. (F) Polymer-drug conjugate controlled release system[279]. (G) a) Bulk degradation and b) surface degradation[264].

2.6 Microspheres

There are various approaches in delivering therapeutic substance to the target site in a sustained and controlled manner. Liposomes, hydrogels, polymer-based discs, rods, pellets or microparticles have been employed to encapsulate drugs which are then released at controlled rates for long periods of time [233, 254, 280-282]. Microspheres are one of the most commonly used carriers for drugs and are advantageous for several reasons, especially when comprised of polymers. Microspheres are small spherical particles with a diameter from 1 to 1000 μm, composed of polymers. Microspheres can encapsulate many types of drugs, including small molecules, proteins and nucleic acids, and are easily administered by serial routes like oral, nasal, transdermal, pulmonary and parenteral injection[282]. They are also generally biocompatible and biodegradable, which can provide high bioavailability and are capable of releasing for sustained periods of time.

2.6.1 Polymers used in biodegradable microspheres

Microspheres can be manufactured from different natural polymers such as gelatin, chitosan, starch or from synthetic polymers such as poly (lactic-*co*-glycolic acid) (PLGA), poly (l-lactic acid) (PLLA), poly (alkyl cyanoacrylates) (PACA)[283, 284]. Figure 5 depicted various biodegradable polymers used in the fabrication of microspheres. Compared to natural polymers, synthetic polymers can be advantageous as they exhibit a higher degree of purity and can be fabricated into different shapes[285, 286]. Additionally, they often offer better control of physicochemical properties. Synthetic polymers are capable of being copolymerized with another to change their mechanical, physical and chemical properties and forming materials with low or high molecular weights using appropriate reaction conditions[243, 287].

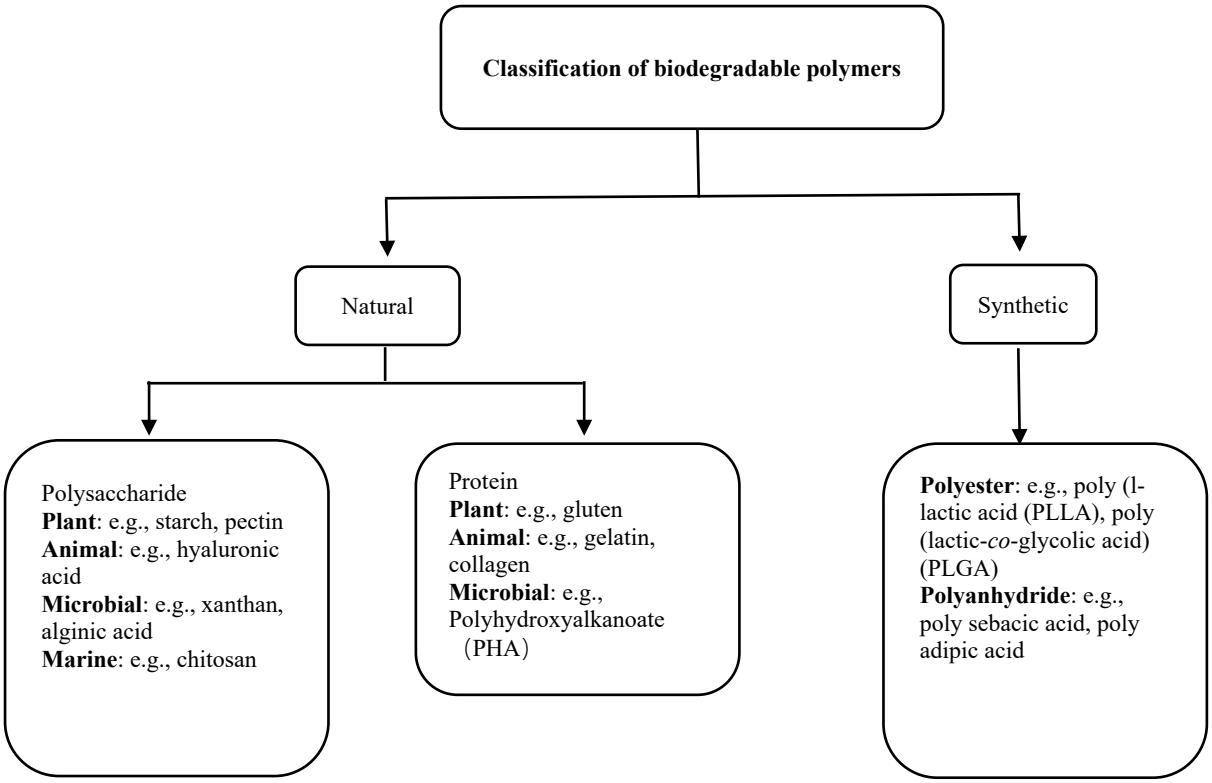

Figure 5. Classification of biodegradable polymers used for preparation of microspheres[288].

Among all polymers, PLGA and PLLA have been mostly used as drug delivery systems and scaffolds for tissue engineering owing to their superior mechanical and processing characteristics[289-291]. Various microspheres based on PLLA and PLGA have exhibited they could carry drugs ranging from small molecules to large proteins as well as DNA and RNA in a sustained release fashion[36, 292-296]. The drug release rate could be easily changed by altering some parameters including molecular weight of polymer, chemical composition of polymer, polymer crystallinity, microsphere size and porosity, drug loading and drug-polymer interaction[257, 297].

PLGA is the copolymer of D, L-lactic acid and glycolic acid, while PLLA is a product polymerized by L-lactic acid because of the chiral nature of lactic acid. Figure 6 and Figure 7 depict the chemical structures of PLGA and PLLA. PLGA and PLLA can be processed into almost any size and shape, while being soluble in many common solvents such as acetone,

ethyl acetate, dichloromethane and trichloromethane[290, 298]. Despite being non-water soluble, they are biodegraded by hydrolysis of their ester linkages in water. PLLA and PLGA have FDA-approved biodegradability and biocompatibility. They are degraded by esterase between the copolymers, leaving lactic acids and glycolic acids entering the tricarboxylic acid cycle to be excreted in the form of water and CO_2 through feces, urine and respiration[299]. As PLLA has hydrophobic side chain (methyl groups), PLLA degrades slower than PLGA, hence the drug would be released faster in PLGA than that from PLLA[290].

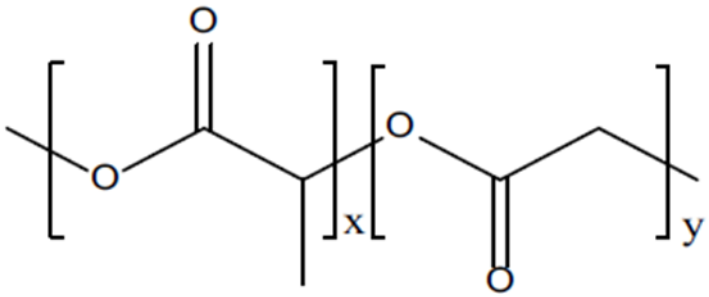

Figure 6. Chemical structure of PLGA (x is the number of units of lactic acid and y is the number of units of glycolic acid)[300].

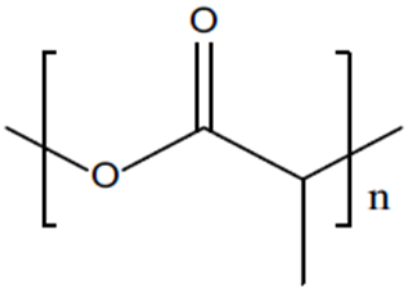

Figure 7. Chemical structure of PLLA[301].

2.6.2 Double-walled microspheres (DWMS)

Conventional microsphere drug delivery systems consisting of one single polymer to encapsulate drugs have numerous drawbacks, including high initial burst release due to drug being trapped on the surface and drug diffused via pre-existing channels and pores in the microspheres, lower encapsulation efficiency and inability to provide sustained release[36, 270, 300, 302]. Microspheres made with shell-core two layers could be an alternative to solve these problems. Double-walled microspheres (DWMS) are composed of two distinct layers as a shell

and a core and are formed through phase separation of two immiscible polymers in solution. DWMS with the drug loaded in the inner core and engulfed by a drug-free outer layer could provide release kinetics with a lower burst release and a longer drug release period than SWMS since the amount of polymer, where the drug must diffuse through, is increased[41, 303-307]. In addition, the stability of drugs can be maintained in the process of dispersing and particle hardening since the drugs are encapsulated within the inner core[43]. The encapsulation efficiency has also been improved to be around 56% for DWMS from 40% for SWMS[308]. In addition, the initial burst was less than 5% and the sustained release lasted for over 3 weeks using DWMS[308]. Navaei *et al.* reported DWMS could encapsulate meglumine antimoniate efficiently up to 87%, decrease initial burst release by 18% and prolong release only 33% after 18 days compared with single-layered microspheres which had 35% burst release and an above 83% release after 18 days[309]. Tan *et al.* also reported increased encapsulation efficiency from about 42% for SWMS to above 75% for DWMS and a sustained release of about 40% over a 4 week period[42].

Over the last decades, there are several methods to fabricate DWMS by dissolving polymers in solvents and precipitating them into spheres such as solvent evaporation[41], solvent removal[310], spray-drying[311], electrospray[312], coacervation process[313]. The solvent evaporation method is extensively developed for the fabrication of DWMS encapsulated with hydrophilic drugs [305, 307, 314, 315]. Tan *et al.* described the fabrication of DWMS based on PLLA and PLGA, where doxorubicin was encapsulated in the core using solvent evaporation[41]. Likewise, Xiao *et al.* successfully fabricated PLGA and PLLA microspheres loaded with aspirin using this method[316]. With solvent evaporation, aqueous solutions of drugs or solid powder of drugs are initially emulsified with one polymer solution, which then is emulsified with the other polymer solution. Subsequently, the emulsion is injected dropwise into the non-solvent water bath composed of a surfactant to form

microspheres. The resulting solution is stirred for a long time to evaporate the solvent until the phase separation occurs between two polymers and the polymer droplets solidify. The microspheres can be harvested by filtration or centrifuge and lyophilized to remove water.

During the process of phase separation, two polymers are most likely configured to have their greatest thermodynamic stability if the solvent evaporation time is extended enough based on spreading coefficient theory[304, 317, 318]. Spreading coefficient theory describes the tendency of a liquid to spread on another liquid when they are dispersed in a third immiscible phase in terms of their interfacial tensions[318-321]. The following equation is to calculate the spreading coefficient for the determination of the ability of one polymer to engulf the other:

$$\lambda_{AB} = \gamma_{BS} - \gamma_{AS} - \gamma_{AB} \quad (1)$$

Where γ_{AS} and γ_{BS} are the interfacial tensions between the solvent and polymer A or B, respectively, and γ_{AB} is the interfacial tension between the polymer A and B. Given the spreading coefficient is positive, polymer A will spread onto polymer B[318]. There are three possible configurations of the two polymers, complete engulfment, partial engulfment and non-engulfment as shown in Figure 8. Nevertheless, the spreading coefficient is only an indirect evaluation of the final configuration of particles before the polymer solutions precipitate since as the polymer concentrations change during the evaporation, the interfacial tensions change, causing to the spreading coefficient constantly changes [317, 322]. In addition, the polymer emulsion droplets are less and less mobile during the solvent evaporation process until they do not have enough mobility to form internal configurations.

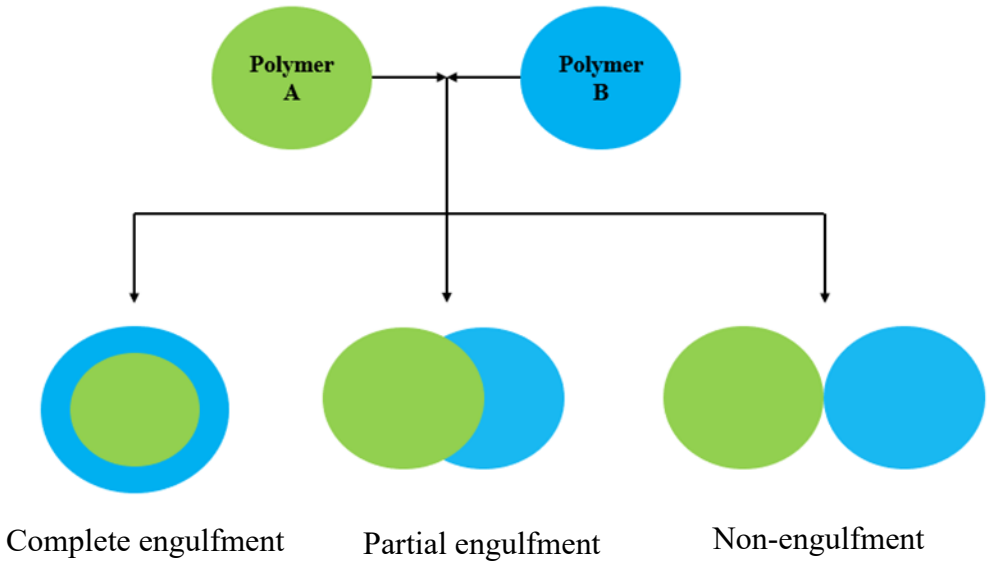

Figure 8. Three possible configurations for the two-polymer system: complete engulfment, partial engulfment and non-engulfment[318, 320].

Ideally, the release of drugs from DWMS can be divided into three phases[282, 306, 317]. Initially, there is a very low or no initial burst release of the drug. Subsequently, a very slow or no release period, known as the lag phase where diffusion is limited. The duration of this period is determined by the microsphere porosity, drug size, polymer degradation kinetics and potential interactions of the drug with polymers. Finally, a large portion of drugs are released quickly after the bulk degradation of polymers. The drug release duration could vary from a few hours to many months.

2.6.3 Use of microspheres for stroke treatment

Microspheres can be administered through injection or embedded within hydrogels or constructs as drug delivery vehicles for prevailing biomedical applications. Table 2 summarises some of the studies based on polymer microspheres used in drug delivery systems to improve outcomes after stroke.

Table 2. Summary of several microsphere for treatment of stroke

Microsphere format	Encapsulated drug	Administration	Therapeutic effects	Reference
PLGA microparticles incorporated into HAMC gel	Cyclosporin A (CsA)	HAMC containing CsA-loaded PLGA microspheres was placed on the brain cortex of adult mice	Detected local release of CsA in the niche at a constant concentration for 3-4 weeks post-implant and promoted NPCs survival	[323]
PLGA microspheres mixed with HA hydrogels	VEGF and angiopoietin-1 (Ang1)	Implanted into the injured cavity of mouse model with MCAO	Strong compatibility with the brain tissue and inhibition to inflammation and gliosis after implantation, enhanced angiogenesis around ischemic regions and improved behavioral improvement	[324]
PLGA-PLLA-PEG microsphere	BDNF	Drug release was performed *in vitro* and bioactivity of BDNF was tested using PC12 cells	The system released bioactive BDNF consistently without an initial burst, and the delivery lasted greater than 60 days	[325]

Gelatin microspheres	Osteopontin	Intrastriatal administration to rat model with transient MCAO at 1-12h post-stroke	Reduced infarct volume, enhanced neuroprotective potency, and prolonged the therapeutic window to over 12h post-MCAO	[326]
Collagen-alginate microspheres	FGF-2	Injection into zebrafish embryos and subcutaneously into mice	No inflammatory reactions; induced progressive and sustained release for over a week and enhanced vascularization	[327]
PLGA microparticles	Fenofibrate	Intracerebral administration to rats 24 hours before MCAO	Released for over seven days and reduced the infarct size in stroke rats	[328]
PLGA microspheres	ONO-1301 prostacyclin agonist	Subcutaneous injection and oral administration immediately after transient MCAO in rat models	Improved neurological deficit scores, decreased oedema and infarct volume, and sustained release for about 3 weeks	[329]
Gelatin hydrogel microspheres	Insulin-like growth factor (IGF) and hepatocyte growth factor (HGF)	The administration was stereotaxically injected into the striatum of mice after 11 days of MCAO	Microspheres containing IGF-1 improved the survival of new neurons in the SVZ; Microspheres containing HGF improved the migration of new	[330]

			neurons from the SVZ to the injured striatum.	
PLGA microparticles	NSCs	Direct injection into the lesion cavity of rats two weeks after MCAO	Successful NSCs attachment with high density, viability and stem cell properties, a primitive *de novo* tissue formed within seven days after implantation	[331]
Poly (ester amide) (PEA) microspheres	VEGF	Intracerebral injection into mice subjected to cortical stroke	Reduced inflammatory response after stroke, promoted angiogenesis, and improved functional recovery	[332]
Gelatin microspheres	bFGF	Stereotaxical injection into rat brains 7 days after MCAO	Aid neovascularization around the transplanted region, promoted survival and proliferation of NSCs, significantly enhanced histological and functional recovery	[333]
Gelatin microsphere	High mobility group box 1 (HMGB1)	Intracranial administration into the striatum of rats with MCAO	Reduced infarct volume, remarkable improvement of neurological deficits, supressed inflammatory	[334]

			effects, extended the therapeutic window to 6h post-MCAO	

2.7 Scope of this study

2.7.1 Motivation

The motivation regarding this project was to provide a state-of-the-art treatment for stroke by designing a novel drug delivery system which can overcome the clinical impracticality of current treatments. The design was achieved by reviewing several fields currently undergoing research for stroke treatment options, including biodegradable synthetic polymers, drug delivery systems and endogenous stem cell therapies. Since the duraplasty is often applied to replace and repair the dura mater layer of the brain after DC, it creates a convenient opportunity to place a drug delivery system in the brain simultaneously. The drugs to be delivered, specifically growth factors, would be released in a sustained manner, inducing endogenous neurogenesis and improving recovery after stroke.

In this thesis, we hypothesize that the PLLA and PLGA DWMS loaded with drug would be a useful drug delivery system to provide a sustained and controlled drug release profile suitable for stimulating endogenous regeneration for stroke treatment.

2.7.2 Objectives

These are the following objectives we plan to achieve for this thesis:

Aim 1: Prepare and optimize the fabrication of DWMS.

Aim 2: Characterize the DWMS including morphology, size analysis, layer analysis by using scanning electron microscope (SEM) images, thermal analysis by using differential scanning calorimetry and encapsulation efficiency.

Aim 3: Investigate the localization of the drug by using fluorescent microscopy (FM).

Aim 4: Evaluate the drug release profile of the DWMS.

3. Materials and Methods

3.1 Materials

Poly (l-lactic acid) (PLLA, inherent viscosity: 0.90-1.20 dL/g), poly (lactic-*co*-glycolic acid 50:50) (PLGA, inherent viscosity: 0.76-0.94 dL/g) were purchased from Durect Corporation (Cupertino, CA). Bovine serum albumin (BSA, Mw 66.5 kDA) was purchased from MP Biomaterials, Inc (Solon, OH). Poly (vinyl alcohol) (PVA, Mw 9,000-10,000 g*mol^{-1}, 80% hydrolyzed) was purchased from Sigma-Aldrich (Burlington, ON). Analytical grade dichloromethane was purchased from Fisher Scientific Company (Ottawa, ON). Phosphate buffer saline (PBS) used for *in vitro* release study was obtained from Amresco Biochemicals and Life Science® (Solon, Ohio) containing 137 mM NaCl, 2mM KCl and 10 mM phosphate buffer. 0.01 % w/v analytical grade sodium azide was added to the PBS, obtained from BDH Chemicals (Mississauga, ON). N-hydroxysuccinimide (NHS)-Rhodamine (Mw 528g*mol^{-1}, Thermo Scientific, USA) was used as per the manufacturer's instructions. All other materials and solvents used were of analytical grade and without modification unless otherwise indicated.

3.2 Methodologies

3.2.1 Preparation of blank double-walled Microspheres (DWMS)

Double-walled microspheres were fabricated by a modified oil-in-oil-in-water (O/O/W) emulsion solvent evaporation method as reported by Tan *et al.*[41] with minor modifications. In brief, 0.15g PLLA and 0.15g PLGA were dissolved in 1ml dichloromethane (DCM) separately. The 15% w/v PLLA solution was slowly added to the 15% w/v PLGA solution to achieve PLLA and PLGA mass ratio of 1:1. The resulting mixture was homogenized using an OMNI homogenizer (Kennesaw, GA) at a speed of 33000 rpm for 90s to create an O/O (oil-in-oil) emulsion, which was immediately added dropwise to a 200ml 0.5% w/v PVA aqueous solution to form an O/O/W (oil-in-oil-in-water) emulsion. The O/O/W emulsion was stirred at 500rpm for 4h at room temperature to evaporate the organic solvent using a Caframo BDC2002

mechanical stirrer (Georgian Bluffs, ON). Subsequently, the resulting microspheres were extensively washed to remove residual PVA and lyophilized for 3 days. Blank DWMS having different PLLA and PLGA mass ratios (w/w) from 1:1 to 1:3, were all prepared for characterization and comparison. The conditions for fabricating blank microspheres in different formulations are demonstrated in Table 3 from F1 to F9.

Table 3. Formulations of DWMS

Formulation code	PLLA/PLGA mass ratio	Polymer concentration (w/v %)	Stirring speed (rpm)	Solvent evaporation time (hrs)	PVA concentration (w/v %)	Addition form of BSA
F1	1/1	20	500	4	0.5	—
F2	1/1	15	500	4	0.5	—
F3	1/1	10	500	4	0.5	—
F4	1/1	15	500	12	0.5	—
F5	1/1	15	500	4	1	—
F6	1/2	15	500	4	0.5	—
F7	1/3	15	500	4	0.5	—
F8	1/1	15	700	4	0.5	—
F9	1/1	15	1000	4	0.5	—
F10	1/1	15	500	4	0.5	Solid
F11	1/1	15	500	4	0.5	Solution
F12	1/2	15	500	4	0.5	Solid
F13	1/2	15	500	4	0.5	Solution
F14	1/3	15	500	4	0.5	Solid
F15	1/3	15	500	4	0.5	Solution

3.2.2 Preparation of rhodamine-BSA particles

Rhodamine-BSA was prepared by using the example protocol for antibody labeling with NHS-Rhodamine from the Thermo Scientific manufacturer instructions. To label BSA with fluorescent rhodamine, NHS-rhodamine was dissolved in DMSO to obtain a 10mg/ml solution. 158.4 µl of this solution was gradually mixed with 2 ml of 10 mg/ml BSA in PBS (pH 7.2), and the reaction mixture was well mixed and allowed to react for 1 h at room temperature under constant agitation. Subsequently the reaction mixture was purified using a dialysis tubing (MWCO 12,000-14,000) (Fisher Scientific, Ottawa, ON). Finally, the purified rhodamine labelled BSA was lyophilized and then mixed with BSA at a mass ratio of 1:500 (labelled *vs.* unlabeled).

3.2.3 Preparation of BSA loaded double-walled microspheres (DWMS) with different polymer ratios

The BSA loaded DWMS were prepared using W/O/O/W (water-in-oil-in-oil-in-water) and S/O/O/W (solid-in-oil-in-oil-in-water) emulsion solvent evaporation method. In the W/O/O/W method, at 1:1 PLLA and PLGA mass ratio, 0.3g PLGA was dissolved in 2ml DCM and emulsified with 0.4ml aqueous BSA solution (75mg/ml) using magnetic stirrer (300rpm for 1h). This emulsion was homogenized for 90s at 33000 rpm and sonicated using a Branson sonicator (Fisher Scientific, Ottawa, ON) for 5 minutes. The processed emulsion was added to 2ml DCM solution of PLLA (15% w/v) and homogenized for an additional 90s at 33000 rpm to form an BSA-PLGA-PLLA emulsion. This mixture was slowly injected dropwise into a 400ml aqueous solution of 0.5% w/v PVA. The mixture was stirred at 500rpm for 4h at room temperature to completely evaporate the organic solvent using the Caframo BDC2002 mechanical stirrer (Georgian Bluffs, ON). Finally, the resulting microspheres were extensively washed to remove residual PVA and lyophilized for 3 days. In the situation of S/O/O/W microspheres, at 1:1 PLLA and PLGA mass ratio, 30mg of BSA powder was used instead of

the BSA aqueous solution. The W/O/O/W and S/O/O/W microspheres at 1:2 and 1:3 PLLA and PLGA mass ratios were also fabricated with changes of adding BSA aqueous solution or BSA powder to PLLA solution first, which was followed by mixing with PLGA solution instead. The process is displayed in Figure 9. The conditions for preparing BSA loaded microspheres in different formulations are demonstrated in Table 3 from F10 to F15.

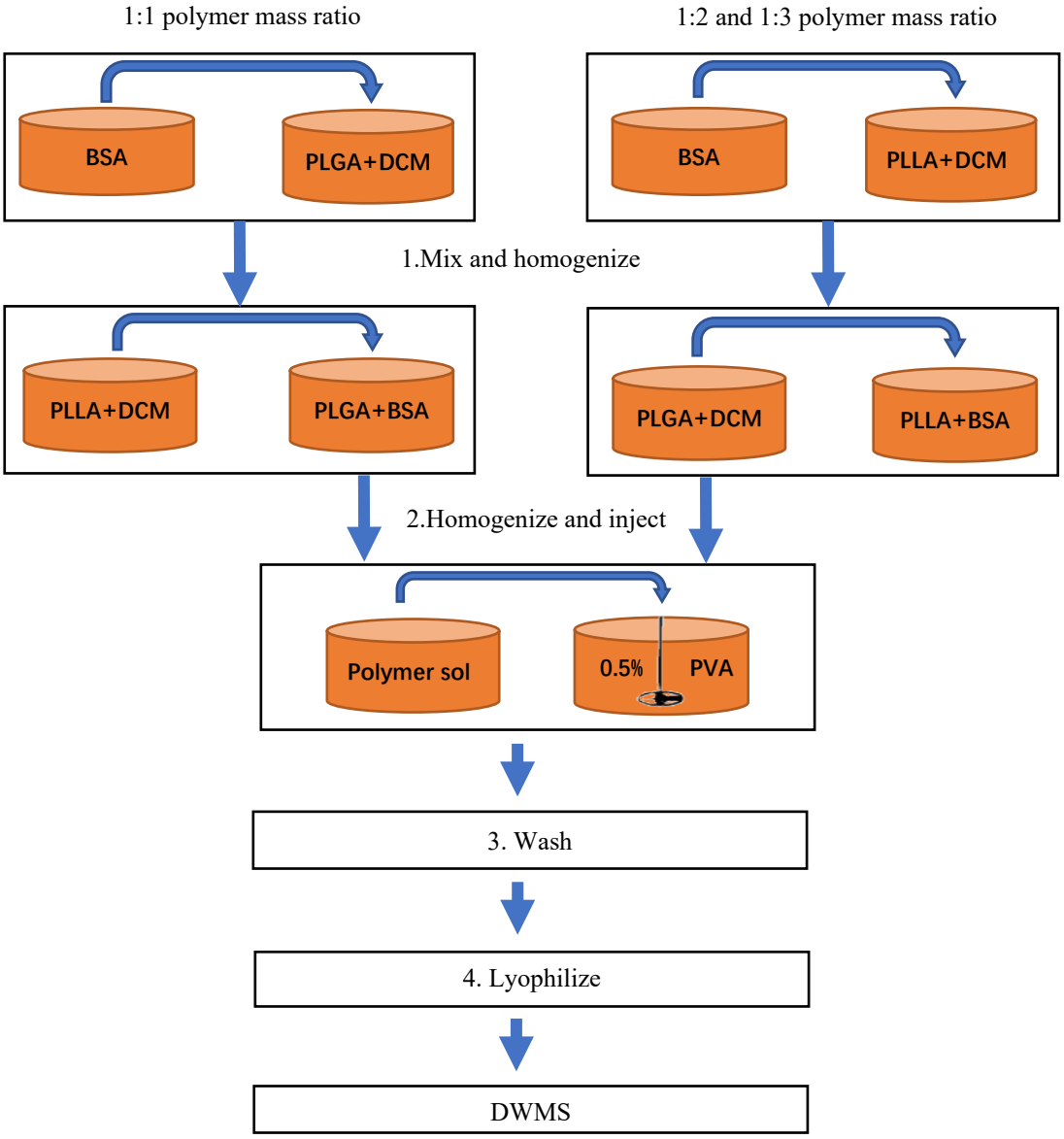

Figure 9. Schematic of BSA loaded DWMS fabrication.

3.3 Characterization

3.3.1 Microspheres yield

Microspheres recovered at the end of the preparation procedures were weighed and the yield was calculated based on the following equation:

$$Microsphere\ yield\ (\%) = \frac{mass\ of\ recovered\ microspheres}{mass\ of\ polymer\ and\ drug\ initially\ used} \times 100\% \quad (2)$$

3.3.2 Morphology of microspheres

The DWMS morphology was observed by scanning electron microscope (SEM, Phenom Pro, Phoenix, AZ) at an accelerating voltage of 15kV. To characterize the core-shell structure of the DWMS, the microspheres were first embedded into OCT embedding compound (Fisher Scientific, Ottawa, ON) at -20 ºC and then cryo-sectioned at a thickness of 40 μm using a Leica CM3050S cryostat (Richmond Hill, ON) to expose the cross-sectional area for internal structure investigations by SEM.

3.3.3 Microsphere Size Analysis

To study the particle size of DWMS, SEM images of the DWMS were analyzed using NIH ImageJ (Bethesda, MD). Both BSA-loaded and blank microspheres were analyzed.

3.3.4 Double-walled microspheres (DWMS) core-shell layer analysis

The chemical compositions of the core and shell polymers in DWMS were studied using a dissolution method. This method takes advantage of different solubilities of PLLA and PLGA in ethyl acetate (EA) – PLLA is insoluble in EA whereas PLGA is soluble in EA – to identify the core and shell materials under different formulations and fabrication processes[41, 309, 335]. Specifically, DWMS were also first embedded into OCT embedding compound (Fisher Scientific, Ottawa, ON) at -20 ºC and cryo-sectioned at a thickness of 40 μm using a Leica CM3050S cryostat (Richmond Hill, ON) and the sectioned samples were mounted onto SEM stubs with double-sided carbon tapes. Subsequently, a total of 1 ml EA was carefully and

slowly pipetted onto the cryo-sectioned microspheres mounted on the SEM stubs to immerse the samples for dissolution with no agitation. Finally, the samples were carefully air-dried and imaged under the SEM.

3.3.5 Encapsulated growth factor distribution inside of double-walled microspheres (DWMS)

The distribution of the encapsulated growth factor inside of the DWMS was investigated by encapsulating fluorescently labelled BSA (i.e., rhodamine-BSA) into the DWMS and studied the distribution of the rhodamine-BSA inside of the microspheres (i.e., sectioned) using a X81 Olympus fluorescence microscope (Richmond Hill, ON).

3.3.6 Encapsulation Efficiency

The encapsulation efficiency (EE) is referred to as the ratio of actual to theoretical loading of the drug within the microspheres as shown in the following equation:

$$Encapsulation\ efficiency(\%) = \frac{M_{actual}}{M_{theoretical}} \times 100\% \quad (3)$$

Where M_{actual} (mg) is the actual amount of drug experimentally retrieved from a given number of microspheres, and $M_{theoretical}$ (mg) is the theoretical loading of the drug from the same given number of microspheres. To experimentally evaluate M_{actual}, a well-established method was used with minor modifications[304, 307, 309]. Specifically, 20mg microspheres were added to 5 ml of 0.1 M NaOH and incubated for 48 hours at 37 °C to completely degrade the polymers and retrieve the BSA. The resulting solution was then centrifuged at 1000rpm for 5min, and the supernatant was collected to determine the BSA amount (i.e., M_{actual}) using a Pierce BCA Protein Assay Kit following the vendor's protocol (Waltham, MA). Experiments were conducted in triplicate.

3.3.7 Differential scanning calorimetry (DSC)

Thermal analysis of the microspheres was conducted using a differential scanning calorimetry (DSC, DSCQ1000, TA Instruments, New Castle, DE) using nitrogen as a purging

gas to determine glass transition temperatures (Tg). Approximately 5mg of BSA loaded microspheres and blank microspheres were weighed separately into aluminum pans and hermetically sealed with aluminum lids, accompanied with empty hermetically sealed aluminum pans with lids. All measurements were performed to equilibrate for 3 minutes at -20℃ to ensure isothermal starting conditions. Afterwards, they were subjected to a heating system from -20 to 200℃, which was subsequently quench-cooled to -20℃ and reheated again to 200℃. All the heating was applied at a rate of 10℃/min. The resulting thermograms were processed on TA universal analyzer software where Tgs were identified.

3.3.8 *In vitro* release studies

In order to evaluate growth factor release performances, 20mg BSA loaded DWMS were submerged in 2 ml PBS (pH 7.4) releasing buffer with 0.01% NaN_3 and incubated at 37℃ under gentle and constant shaking[336]. At predetermined time points, samples were centrifuged and 1ml of the releasing buffer was removed and replenished same amount of fresh PBS (pH 7.4) with 0.01% NaN_3. To evaluate the BSA concentrations of the collected samples overtime, Pierce BCA Protein Assay Kit was used, and Equation (4) was used to calculate the cumulative amount of BSA released:

$$R = (c_n * v_o) + \sum_{i=1}^{n-1}(c_i * v_i) \quad (4)$$

Where R is the cumulative amount of BSA released at each time point, c_n is the measured concentration from the BCA assay, v_o is the total volume of the sample at that time point, c_i are all the previously measured concentrations from the BCA assay, and v_i are the aliquot volumes (i.e., 1 ml in this study) which were removed from the sample at each time point.

3.3.9 Statistical Analysis

The results are shown as mean ± standard deviation. All the data were statistically analysed using a one-way and two-way analysis of variance (ANOVA). A statistically

significant difference was considered at $p < 0.05$. Statistical analysis was conducted by using GraphPad Prism 6 Data (Graphpad Software, La Jolla, CA).

4. Results and Discussion

4.1. Formation and yield of double-walled microspheres (DWMS)

Our group previously fabricated PLLA and PLGA DWMS by using 20% polymer concentration and 4 h of solvent evaporation time. In this method, the yield was 29.66±1.90%, which was too low to expand production. This low yield was mainly due to the loss of polymers during transfers such as viscous polymers sticking to container walls, and polymers adhering to agitator blades. Moreover, the distribution of BSA within the microsphere remained unknown. To solve these problems and optimize the manufacturing conditions of DWMS, five process variables were studied: polymer concentration (20%, 15%, 10% w/v), polymer mass ratio (1:1, 1:2, 1:3 w/w), solvent evaporation time (4h, 12h), mechanical stirring speed (500rpm, 700rpm, 1000rpm), and PVA concentration (0.5%, 1% w/v). These variables were chosen since they turned out to affect the formation of microspheres by changing the initial properties of polymer solution (concentration, mass ratio) or the conditions of solvent evaporation procedure (time, stirring speed and PVA concentration)[284, 337-339]. These changes could have a great effect on the yield, morphology of microspheres and entrapment of the drug inside the system.

According to Rahman and Mathiowitz[303], the concentration at which the PLLA and PLGA separate into two immiscible phases was 30% w/v, otherwise referred to as the cloud point. Moreover, the polymer mass ratio did not affect the phase separation point. For this reason, the PLLA and PLGA homogeneous polymeric miscible solutions in DCM at below their critical polymeric concentrations (i.e., 10%, 15%, and 20%, w/v) were used to form an O/O emulsion and dispersed into an aqueous PVA solution with mechanical stirring that ultimately led to an O/O/W emulsion. The DCM from polymer solutions were lost by

evaporation, leading to an increased polymer concentration. When the polymer concentration reached and surpassed the critical concentration, a phase separation occurred with the first polymer rich in one phase and the second polymer rich in the other phase. These two polymers eventually hardened to form the DWMS by solvent evaporation.

Table 4. Yields of microspheres in different formulations

Sample	PLLA/PLGA mass ratio	Polymer concentration (w/v %)	Solvent evaporation time (h)	PVA concentration (w/v %)	Microspheres yield (% ± SD*)
F1	1/1	20	4	0.5	29.66±1.90
F2	1/1	15	4	0.5	48.25±5.47
F3	1/1	10	4	0.5	45.13±2.20
F4	1/1	15	12	0.5	39.18±5.72
F6	1/2	15	4	0.5	39.90±1.53
F7	1/3	15	4	0.5	44.97±7.08

*SD = Standard deviation, n=3.

The yields of microspheres in different concentrations (F1, F2, F3) and solvent evaporation time (F2, F4) are shown in Table 4. The results showed that the yield of microspheres prepared in polymer concentrations (20%, 15%, 10% w/v) were 29.66±1.90%, 48.25±5.47%, 45.13±2.20%, respectively. A statistically significant difference ($p<0.05$) in yields was shown from 20% polymer concentration with 15% and 10% polymer concentrations. This agrees with the result from Mufassir *et al.*[340] who report that as polymer concentration increases, the yield of microsphere declines. This is attributed to the increase in polymeric concentration contributing to high viscosity of solution and less time to reach phase

separation[340]. Highly viscous solution results in a larger mass loss during polymer transfers between containers. Rahman *et al.* also reported decreased yield of microspheres as the concentration of HPMC solution increased from 20% to 40% and concentration of Poloxamer solution increased from 10% to 30%[341]. The SEM images of the cross-sectioned DWMS the 20% (F1), 15% (F2), 10% (F3) polymer concentration are shown in Figure 10. The SEM analyses of formulations F1, F2 and F3 prepared had all shown two distinct layers while F1 (Figure 10A) showed uneven, porous surfaces and irregular layers. This might be attributed to fast polymer precipitation resulting from the increased viscosity of polymer[305]. On the contrary, F2 (Figure 10B) and F3 (Figure 10C) showed spherically shaped, non-porous surfaces but the double layer formation of F2 is tighter and denser than that of F3 which showed a distinct gap inferred from the dark barrier between the inner core and outer layer. In this case, by using 15% polymer concentration, DWMS with PLLA and PLGA mass ratios 1:2 and 1:3 were also fabricated. The prepared microspheres (Figure 11) have clearly visible double layers and yielded 39.90±1.53% (F6) and 44.97±7.08% (F7), separately. The yields we obtained were relatively similar to those reported by other researchers. For example, the yield of poly (lactide-*co*-glycolide)-*co*-poly(ethyleneglycol) (PLGA-PEG) microspheres ranging between 28.6% and 66.6% was reported[342]. Kokai *et al*. reported the yield of PLGA and PLLA DWMS was 54.5%[343]. The relatively low yield achieved in this study could be attributed to the losses occurring during steps of processing (i.e., sticking of the polymeric solution to glass containers, loss of microspheres during the washing step).

A relatively prolonged time of mechanical stirring guarantees the complete emulsion of solution, in which utilizes PVA to its full potential. The long stirring time favors the thermodynamic equilibrium orientation of the PLGA and PLLA polymers dictated by conditions such as surface and interfacial tensions[337, 344]. However, the yields of microspheres emulsified for 4 and 12 hours were 48.25±5.47% (F2), 39.18±5.72% (F4), which has no significant difference ($p > 0.05$). The emulsion system remained stable and constant at 4 hours.

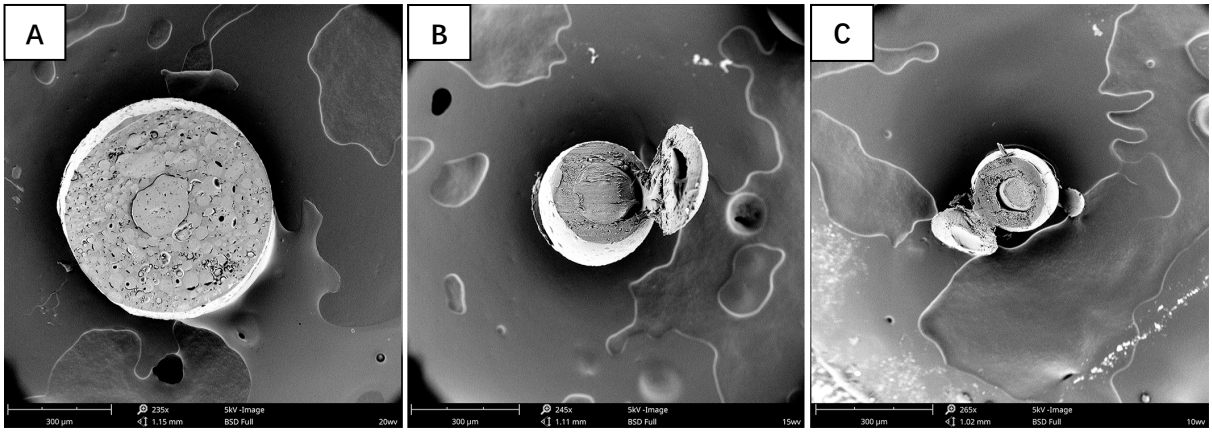

Figure 10. Scanning electron images of cross-sectioned DWMS with polymer concentrations of (A) 20%, (B) 15% and (C) 10% showing two distinct layers.

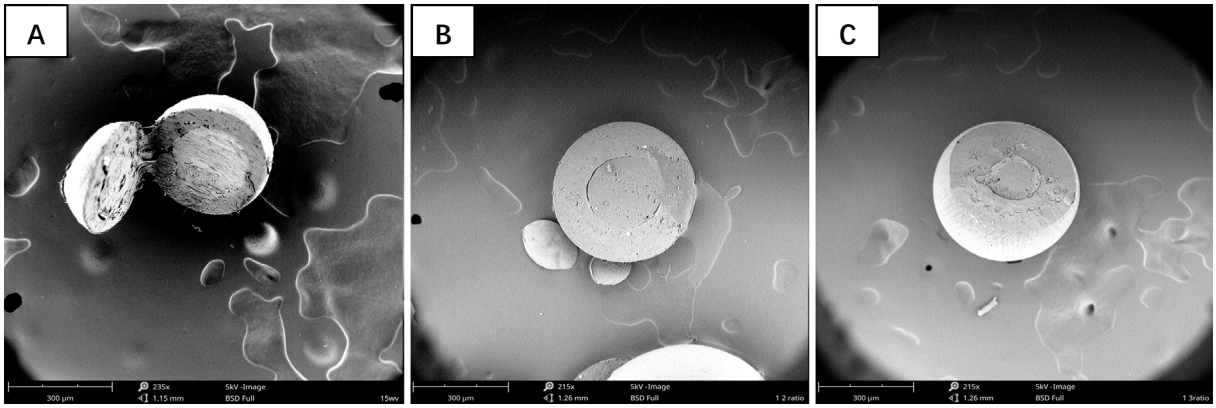

Figure 11. Scanning electron images of cross-sectioned DWMS with polymer mass ratios of (A) 1:1, (B) 1:2 and (C) 1:3 showing two distinct layers.

4.2 Particle size characterization

Size of microspheres is determined by parameters such as mechanical stirring speed of solvent evaporation, viscosity of polymer solution and PVA concentration[345]. Table 5 shows different fabrications of microspheres in polymer concentrations (20%, 15% and 10% w/v)

yielded significantly different mean diameters of 594.17±138.71, 370.51±96.81, 233.42±43.63 μm, respectively, suggesting that concentrations (i.e., 20%, 15%, 10% w/v) used in this study significantly impacted resulting particle diameters ($p < 0.05$) shown in Figure 12C. These results correspond with earlier findings in previously published studies using a similar method for the fabricated microspheres with mean diameters of 30-210 μm[346] and 237-387 μm[347]. The particle size dependence on polymer concentration is likely explained by the viscosity of the polymer solutions as high concentration polymer solutions would translate to high viscosity polymer solutions that require high shearing energy to break the emulsion droplets or result in bigger emulsion droplets at the same shear force[348, 349]. Fabrications of DWMS with PLLA and PLGA mass ratios of 1:2 and 1:3 yielded mean diameters of 305.33 ± 129.01 μm and 355.29 ± 133.32 μm, respectively. With a constant amount of core material, the shell thickness could vary as the PLLA and PLGA mass ratio was altered from 1:1 to 1:3. This is evident in Figures 11A, 11B and 11C where DWMS were fabricated to be relatively large for easy cross-sectioning with the cryostat blade at the centrelines of microspheres with reasonable accuracy. Similar results were also obtained from other researchers. For example, Tan *et al.* produced microspheres at different PLLA and PLGA mass ratio (w/w) from 1:1 to 1:3 having varying shell thickness[41]. Lee *et al*. reported there are variations of shell thickness as a result of the changes of PLLA to PLGA mass ratios from 1:1 to 2.5:1 w/w[335].

The typical mean particle diameters of BSA powder and solution loaded microspheres, prepared in the mass ratio of 1:1, 1:2 and 1:3, are shown in Table 5. Figure 12A shows loading BSA into microspheres significantly increases the size of microspheres ($p < 0.05$). For example, at the polymer mass ratio of 1:1, adding BSA solid powder to microspheres led to greater mean particle diameters of 413.45 ± 147.89 μm from 370.51 ± 96.81 μm. In particular, the mean particle diameters of BSA solution loaded microsphere is 647.91 ± 172.97 μm, which is larger

than the size of BSA solid loaded microspheres. The same situation was also observed in the polymer mass ratio of 1:2 and 1:3. Size of microspheres was found to be increased due to the addition of drug. In addition, the larger mean particle size of drug solution loaded microspheres compared to drug solid loaded microspheres could be due to the presence of drug aqueous solution in the first emulsification of solution loaded microspheres[309].

Table 5. Size of microspheres prepared in different formulations

Sample	Polymer concentration (w/v %)	PLLA/PLGA mass ratio	BSA addition form	Mean diameter (μm ± SD*)
F1	20	1:1	—	594.17±138.71
F3	10	1:1	—	233.42±43.63
F2	15	1:1	—	370.51±96.81
F10			Solid	413.45±147.89
F11			Solution	647.91±172.97
F6		1:2	—	305.33±129.01
F12			Solid	435.21±85.05
F13			Solution	530.17±122.63
F7		1:3	—	355.29±133.32
F14			Solid	436.46±71.94
F15			Solution	587.88±108.08

*SD = Standard deviation, n=100.

It is evident to see from the results that the mechanical stirring speed affects the particle size. Microspheres prepared using 700rpm and 1000rpm resulted in average sizes of 307.93 ±41.38 μm and 49.99±11.02 μm. Compared with the size of microspheres using 500rpm which is 370.51±96.81 μm, the particle sizes are significantly smaller when the stirring speed rises from 500rpm to 1000rpm ($p<0.05$) as shown in Figure 12B. Stirring speed is an important factor since it provides the energy to disperse the oil phase in water[339, 350]. It is the high stirring speed that gives rise to the shear force in the emulsion system, contributing to smaller

emulsion droplets and better dispersion of polymer phase in PVA solution. Our results showed that higher stirring speed yielded smaller size of microspheres since the emulsion was broken into smaller droplets at a higher input power. In another study, the mean diameters of the microspheres were markedly decreased from 251 μm to 104 μm by increasing mechanical stirring speed from 400 to 1200rpm[351].

PVA acted as an emulsion stabilizer between the organic and water phase. The emulsion is formed when the polymer solutions and water are mixed together in high-speed agitation which lead them to form one phase. However, the emulsion is unstable. In this case, PVA is the stabilizer and emulsifier to add in the emulsion. The vinyl chains in PVA interact with the dichloromethane whereas the hydroxyl groups interact with the water phase, hence forming a more stable emulsion. The PVA concentration affects the stability of emulsion, thereby changing the size of microspheres. The presence of higher concentration of PVA in the external water phase stabilizes emulsion droplets against coalescence, leading to smaller emulsion droplets, thus forming smaller microspheres. Nevertheless, an excessive concentration of PVA might cause the fragility of the microspheres and is hard to wash off. In this experiment, when the PVA concentration varied from 0.5% to 1% w/v, the mean diameters of microspheres were decreased from 370.51 ± 96.81 μm to 360.84 ± 147.31 μm, with no significant difference ($p > 0.05$) as shown in Figure 12D. The PVA concentration at this stage, nonetheless, does not appear to affect the final microsphere size.

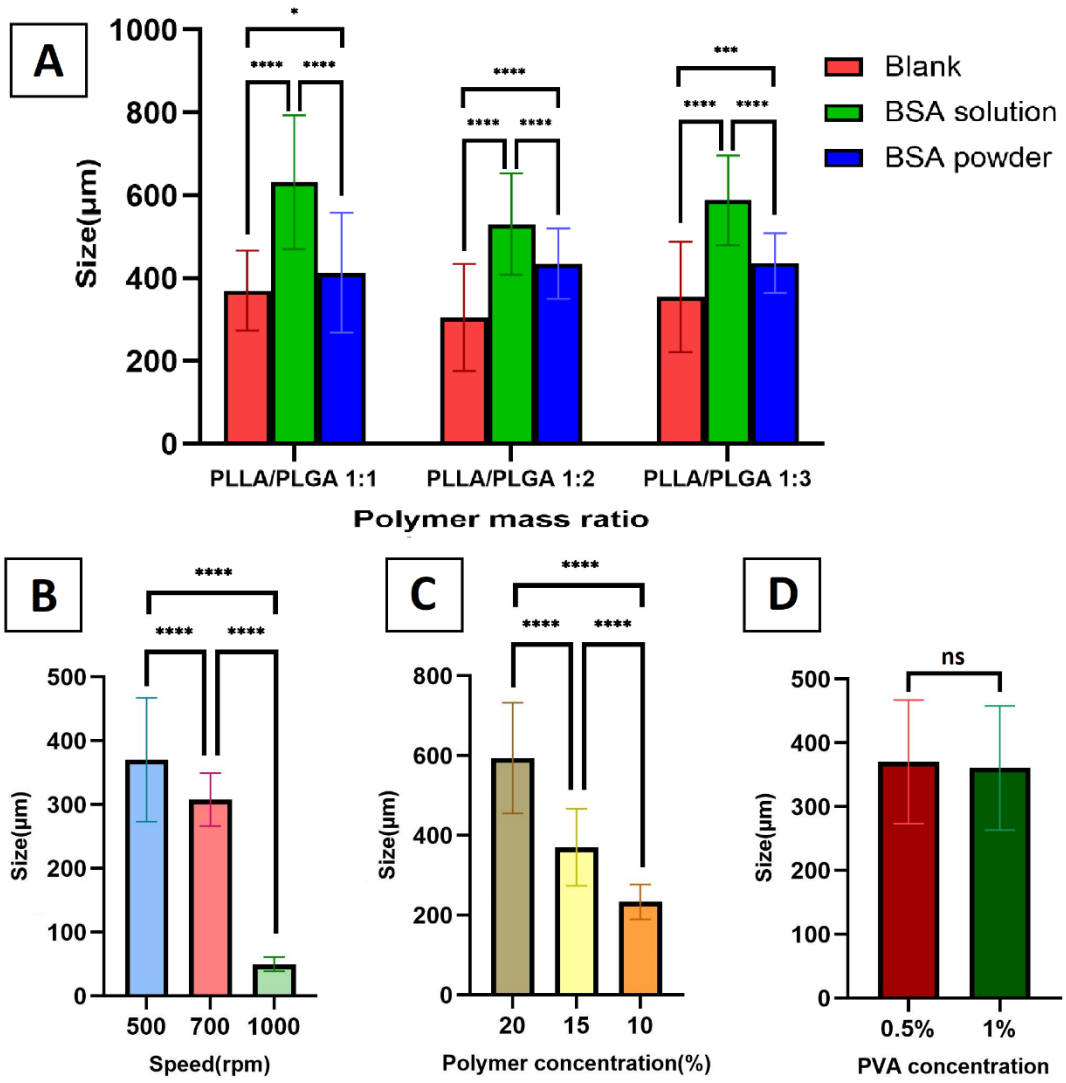

Figure 12. Size analysis of DWMS in different fabrication conditions (n=100, error bars represent standard deviation of the mean): (A) PLLA and PLGA polymer mass ratio from 1:1 to 1:3 at polymer concentration of 15% with different BSA forms loaded. (B) Mechanical stirring speed of 500rpm, 700rpm and 1000rpm at polymer mass ratio of 1:1 and polymer concentration of 15%. (C) Polymer concentrations of 20%, 15% and 10% at polymer mass ratio of 1:1. (D) PVA concentrations of 0.5% and 1% at polymer mass ratio of 1:1 and polymer concentration of 15%.

4.3 Identification of shell and core polymer composition

Cross-sectional images of DWMS with PLLA and PLGA polymer mass ratios from 1:1 to 1:3 after dissolution in ethyl acetate were taken by SEM (Figure 13). Figure 13A and 13B show DWMS with PLLA and PLGA mass ratio of 1:1 having hollow cores with surrounding solid shells which were insoluble in ethyl acetate, whereas Figures 13C,13D and Figures 13E, 13F characterize PLLA and PLGA mass ratio of 1:2 and 1:3, showing solid cores surrounded

by soluble shells dissolved by ethyl acetate. Based on the known solubility of PLGA and insolubility of PLLA in ethyl acetate, the core and shell were identified as PLGA and PLLA with the polymer mass ratio of 1:1. However, after dissolving the microspheres with PLLA and PLGA mass ratios of 1:2 and 1:3, the shells appeared to have dissolved while the core remained. This is because after phase separation, there was a higher quantity of PLGA than there was of PLLA as the PLGA mass increased. The engulfing phase (outer layer) tended to be comprised of the higher mass polymer. This gave us the hint that core-shell inversion occurred when the PLLA and PLGA ratio increased from 1:1 to 1:2. Tan *et al.*[41], Matsumoto *et al.* [352] also reported similar observation of phase inversion in their studies. Therefore, discovering the core and shell material compositions in different polymer mass ratios in advance inspired us to encapsulate drugs specifically in the core material during the fabrication process. Knowing such identifications along with precise prediction of the drug's preferential distribution within two different insoluble polymers allows us encapsulate drugs to be in the inner core to achieve extended drug release.

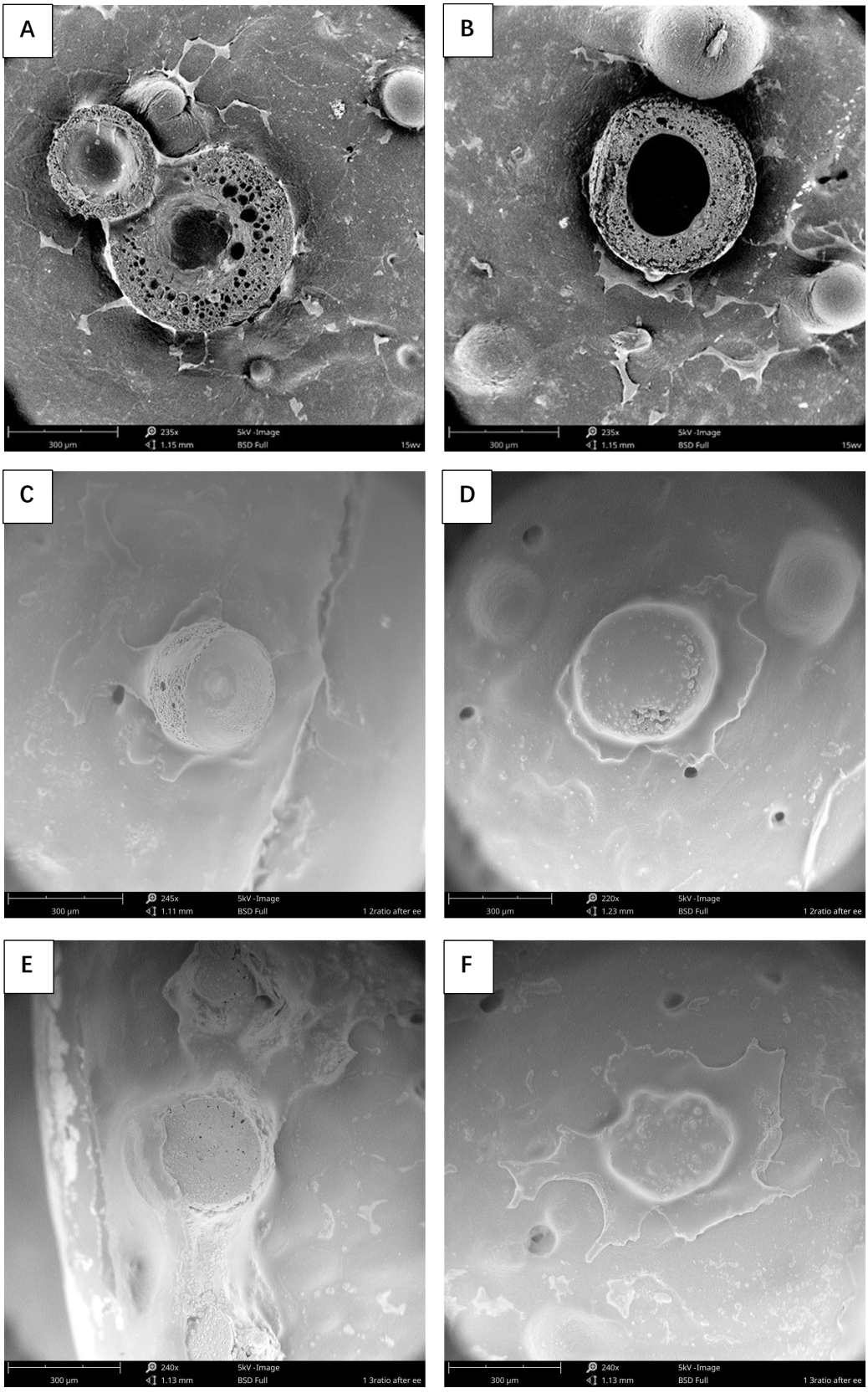

Figure 13. SEM images of cross-sectioned DWMS after washing with ethyl acetate (EA) at polymer mass ratios of (A, B) 1:1, (C, D) 1:2 and (E, F) 1:3 indicate the core and shell of the DWMS.

4.4 Differential scanning calorimetry (DSC) analysis

The fabricated DWMS along with PLGA and PLLA SWMS were examined to determine their Tg by DSC. Tg is the temperature below which the physical properties of polymers change in a manner similar to those of a glassy or crystalline state, and above which they behave in rubbery states. The transition from the glass to the rubber-like state is a significant attribute of polymer behavior, highlighting substantial changes in the physical properties, such as elasticity and hardness. Table 6 shows the respective Tg values of SWMS, blank DWMS and BSA loaded DWMS. There are two separate Tg, one each for PLLA and PLGA in blank double-walled and also BSA loaded DWMS. DSC thermograms identified the points that were plotted together with PLLA and PLGA SWMS used as controls. Two Tgs observed in DSC thermogram indicates two polymers did not form a miscible blend in the DWMS, which means the phase separation of polymers resulting in the formation of double-walled structure occurred.

Table 6. Thermal properties of DWMS and SWMS obtained from DSC thermograms (n=3).

	Literature [335]	PLGA microsphere	PLLA microsphere	Blank DWMS (PLLA/PLGA 1:1)	BSA solution loaded DWMS (PLLA/PLGA 1:1)	BSA solid loaded DWMS (PLLA/PLGA 1:1)
Tg/PLGA (℃)	45-60	47.30±0.40	—	48.40±0.18	47.53±0.15	47.37±0.10
Tg/PLLA (℃)	60-67	—	58.74±0.64	59.40±0.19	59.25±0.37	59.20±0.19

4.5 Identification of BSA distribution

In the pre-encapsulation steps, both the BSA solid and BSA solution were initially placed in the expected inner core material individually (PLGA phase in the polymer mass ratio of 1:1； and PLLA phase in the polymer mass ratio of 1:2 and 1:3). Figure 14 showed that the BSA powder was found to be distributed predominantly in the PLGA layer for these DWMS

regardless of where the PLGA layer is located, both in the core for the case of mass ratio of 1:1 and the in the shell for the mass ratios of 1:2 and 1:3. Our data further suggest that the BSA solid powder always co-localized with the PLGA, whether or not the BSA was first added in the PLGA or PLLA solution before mixing the two polymers together. This means the BSA solid has a higher affinity towards PLGA polymer. Similar selective drug solid distribution in PLGA were also observed by Tan *et al.*[41]. However, the majority of BSA solution always resided within the inner core material with remnants in the shell material from polymer mass ratio 1:1 to 1:3 when the BSA aqueous solution was first emulsified with the core material. The BSA aqueous solution was first emulsified with one polymer solution (core material). Afterwards, the mixture was again emulsified with the other polymer solution (shell material) to form W/O/O emulsion, followed by stirring in PVA solution. This results in DCM evaporates, which causes polymer concentrations to increase until phase separation, and thus double-walled structure were formed. Zheng also observed the similar phenomenon that the hydrophilic drug was localized in the inner polymer layer by pre-emulsifying the drug aqueous solution in the core material[304].

Based on the literatures[317, 335, 353], the drug substance distribution between two polymers varies based on the solubility parameters of the polymer-solvent solutions. The drug substance distribution between two polymer phases is shown as follows: [352],

$$\frac{[Xa]}{[Xb]} = Vs\frac{(\delta s-\delta b)^2-(\delta a-\delta s)^2}{2.3RT} \quad (5)$$

Where [Xa] and [Xb] are concentrations of drug substance S in A phase and B phase, respectively; δa, δb and δs are solubility parameters of A phase, B phase and substance S, respectively; Vs is the molecular volume of substance S; R is the gas constant; and T is absolute temperature. This equation implies that when the substance S exists as a solid state, the distribution of substance S varies depending on the solubility parameters of A phase and B

phase. In our current situation, the equation can be represented as:

$$\frac{[X_{PLGA}]}{[X_{PLLA}]} = V_{drugs} \frac{(\delta_{drug} - \delta_{PLLA-DCM})^2 - (\delta_{PLGA-DCM} - \delta_{drug})^2}{2.3RT} \quad (6)$$

Qualitatively, due to the fact that PLGA and BSA are more polar and hydrophilic than PLLA, we can determine that their solubilities will be more alike than those of PLLA and BSA. Hence, the numerator on the right half side of the equation would be positive. Multiplying by a large positive value of V_{drugs}, the concentration ratio of $\frac{[X_{PLGA}]}{[X_{PLLA}]}$ would be greater than 1, stating the preferential distribution of BSA solid to the PLGA phase, which matches our observations. This theory has already been applied to predict the distribution of etanidazole[335] and doxorubicin[41] in PLLA and PLGA DWMS successfully. However, this drug distribution theory is only applied to drug in solid state[335]. In contrast, the BSA aqueous solution was always localized in the core of DWMS regardless of the core phase material by pre-emulsifying the BSA aqueous solution with the core material. In comparison to the scattered distribution of BSA solid in DWMS, the distribution of BSA solution is denser in the core phase. It is postulated that the immiscible internal water fraction (aqueous BSA solution) encapsulated in the liquid drop (oil phase) form discontinuous regions in the W/O/O emulsions[354]. These discontinuous regions retard the diffusion of solvent from the drop interior to the non-solvent bath. Therefore, the solvent near the drop surface diffuses faster into the non-solvent bath than the solvent from the drop interior. After the phase separation, the oil phase separates into an outer and inner phase. The outer phase pre-solidifies due to the fast solvent removal upon diffusion into the non-solvent bath[304]. Later, the internal water fraction coalesces within unsolidified inner phase[304], forming the localization of aqueous BSA in the inner phase.

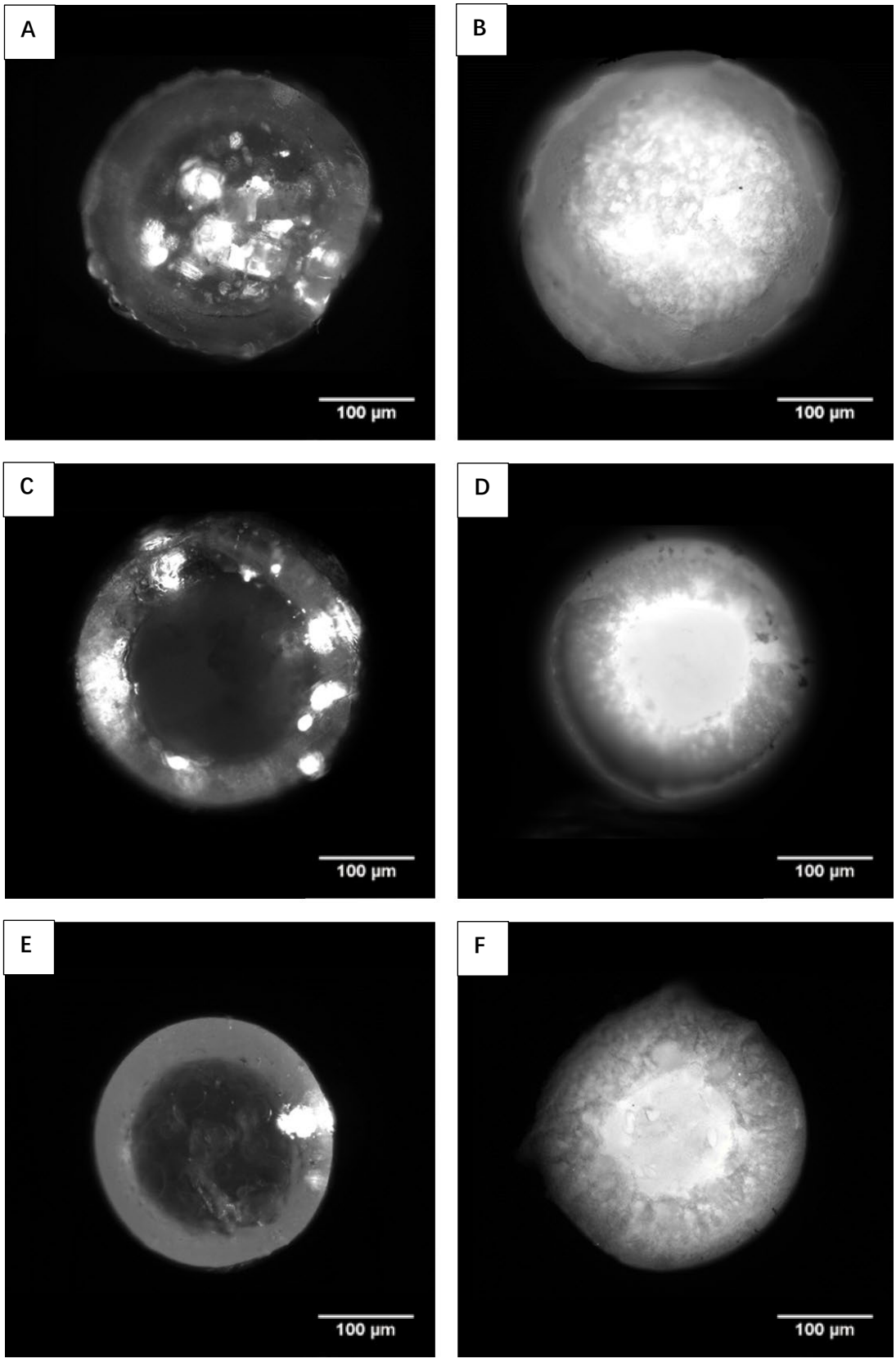

Figure 14. Cross sections of BSA loaded DWMS made from PLLA and PLGA mass ratios of 1:1 to 1:3 under fluorescence microscope. (A) BSA solid loaded DWMS with PLLA: PLGA 1:1. (B) BSA solution loaded DWMS with PLLA: PLGA 1:1. (C) BSA solid loaded DWMS with PLLA: PLGA 1:2. (D) BSA solution loaded DWMS with PLLA: PLGA 1:2. (E) BSA

solid loaded DWMS with PLLA: PLGA 1:3. (F) BSA solution loaded DWMS with PLLA: PLGA 1:3.

4.6 Protein encapsulation efficiency

The encapsulation efficiencies were only tested for the BSA loaded DWMS we successfully yielded after collection. Table 7 showed that encapsulation efficiencies of BSA solid loaded DWMS are 86.66±8.07%, 90.73±2.00% and 85.92±7.54% with the PLLA and PLGA mass ratios from 1:1 to 1:3 with no significance ($p>0.05$). Similarly, by using BSA aqueous solution, high encapsulation efficiencies of up to 90.76±5.75% from PLLA and PLGA mass ratios of 1:1 to 1:3 were achieved with no significance ($p>0.05$). These BSA aqueous solution loaded DWMS compared to BSA solid loaded DWMS, showed no statistically significance ($p>0.05$) in encapsulation efficiency. These values of encapsulation efficiency are higher than that using the original method (15.78±3.62% in SWMS and 26.20±5.83% in DWMS) from our lab and similar to those described by other authors: Tan and Ye attained a low encapsulation efficiency of approximately 42.01% for SWMS and increased that to above 70% using drug solids into DWMS[42]. Wang attained encapsulation efficiency of over 80% using water solution as drugs into DWMS[304]. In DWMS, the drug-free outer layer acts as an additional diffusion barrier inhibiting the drug from leaking out during the microsphere fabrication process, resulting in high encapsulation efficiency. Whereas in SWMS, a low encapsulation efficiency is often achieved due to having only a single diffusion barrier to retain the drugs in the core.

Table 7. Comparison of encapsulation efficiency of different formulations

Sample	Encapsulation efficiency (% ± SD*)
F10; BSA solid loaded DWMS (1:1, w/w)	86.66±8.07%
F11; BSA solution loaded DWMS (1:1, w/w)	83.81±4.00%
F12; BSA solid loaded DWMS (1:2, w/w)	90.73±2.00%
F13; BSA solution loaded DWMS (1:2, w/w)	89.70±5.31%
F14; BSA solid loaded DWMS (1:3, w/w)	85.92±7.54%
F15; BSA solution loaded DWMS (1:3, w/w)	90.76±5.75%

*SD = Standard deviation, n = 3.

4.7 *In vitro* BSA release

The cumulative BSA release from the DWMS was investigated *in vitro* for a 21-day period and the relation between the cumulative release amount and releasing time was plotted in Figure 15. The DWMS with BSA solid loaded in the inner core (PLLA and PLGA mass ratio of 1:1) and outer layer (PLLA and PLGA mass ratios of 1:2 and 1:3) were compared to DWMS with BSA solution loaded in the inner core (PLLA and PLGA mass ratios of 1:1 to 1:3). As of 21 days, 20mg of the BSA solid loaded DWMS showed cumulative releases of 43.88±5.47, 196.71±18.69 and 152.61±24.18 μg from PLLA and PLGA mass ratios of 1:1 to 1:3 and the 20mg of the BSA solution loaded DWMS showed cumulative releases of 562.09 ±42.46，676.30±48.78，699.55±48.60 μg from PLLA and PLGA mass ratios of 1:1 to 1:3. The release testing of the BSA solid loaded DWMS are all less than 20% within 21 days. In contrast, BSA solution loaded DWMS released up to 77.08%, sparking a speculation for an earlier plateau in the BSA solution loaded DWMS. This might be due to the distribution of drugs in solution forms inside the polymer is more uniform compared to dispersion of drug solid, hence the drug release profiles are improved. Due to such a high difference in BSA release, the BSA solid loaded DWMS and BSA solution loaded DWMS will complete their releases at different time frames. The cumulative release profiles showed decreased initial burst of BSA solid loaded DWMS compared with BSA solution loaded DWMS. It is postulated that,

BSA solid loaded DWMS experienced slight initial bursts, which followed by lag phases within 21 days as Figure 15 demonstrated; the release will continue to increase for a period of time until a plateau (where no further release is seen) occurs. It is likely that more time is needed before this trend will be observed. While the release profiles of BSA solution loaded DWMS in polymer mass ratios of 1:1 to 1:3 had a similar trend where half the amount of BSA burst within 4 days. From this, it is likely that the BSA solid loaded DWMS can be expected to continue to release for a longer period of time than the BSA solution loaded DWMS.

The release profile in Figure 15 also showed that the microspheres made from polymer mass ratios of 1:2 and 1:3, with the BSA solid localized in the outer layer, had higher burst release and total release compared to DWMS made from polymer mass ratio of 1:1 with BSA solid localized in the inner core. The PLLA shell of DWMS when PLLA and PLGA mass ratio was 1:1, performed as a barrier and effectively inhibited the drug diffusion from the PLGA core. The BSA solid was located in the outer layer when PLLA and PLGA mass ratios were 1:2 and 1:3, leading to improved release within the same period. It also can be seen that, at polymer mass ratio of 1:2 or 1:3, even if the BSA solid was localized in the outer layer of DWMS, while the BSA solution was localized in the inner core, the BSA still released faster from BSA solution loaded DWMS than that from BSA solid loaded DWMS. According to literature, this is to be expected because inner BSA water droplets may tend to coalesce with each other in the double emulsion and form interconnected water channels during the period of solvent removal by partial droplet coalescence[350, 355]. During the formation of double emulsions, the water is driven by osmosis pressure to penetrate from external water phase into internal water phase, resulting in the formation of interconnected channels[356]. The droplet coalescence and formation of interconnected channels were inhibited to some extent by the stabilization of PVA in the external water phase, and thus prevent too much loss of BSA being encapsulated from diffusion towards the external water phase[355]. These water channels

appear as pores after hardening of the microspheres[305, 356]. This causes drug aqueous solution loaded DWMS to be porous as reported elsewhere[350, 357, 358]. The drug diffuses through the pre-existing interconnecting pores or channels of microspheres resulting in an increased release rate of BSA.

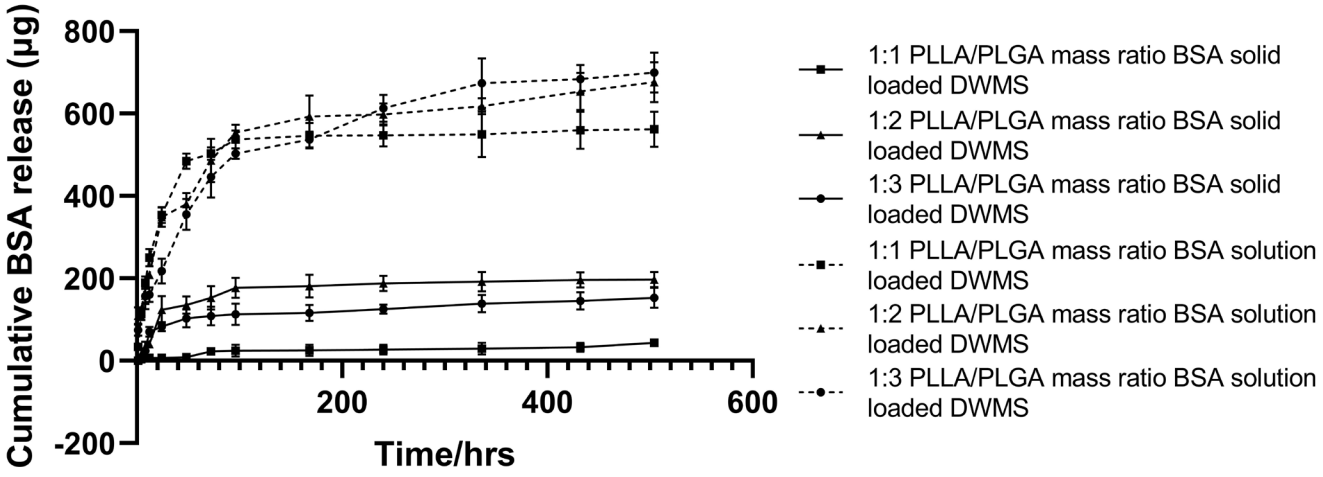

Figure 15. Cumulative release profile of BSA from DWMS (n=9, error bars represent standard deviation of the mean).

The analysis of drug release kinetics was conducted by fitting the plotted cumulative release data to time with an exponential equation: zero order kinetics, first order kinetics, Higuchi's square root of time equation and semi-empirical equation proposed by Korsmeyer-Peppas. The release models which best fitted the release data were evaluated by correlation coefficient (R^2) obtained from release data of various formulations.

Zero order model defines the process of constant drug release from a drug delivery system and drug level in the media. It refers to a system with its drug release rate independent of the dissolved substance concentration[269, 275, 359, 360]. Zero order model can be represented by the equations below:

$$Q_t = Q_0 + K\,t \tag{7}$$

Q_t is the cumulative amount of drug released at time t, Q_0 is the initial amount of drug, usually equal to zero, K is the zero-order release constant, t is the time in hours.

First order model defines the release from system where release rate is dependent on concentration [361, 362], expressed by equation (8):

$$Q_t = Q_0 e^{-Kt} \quad \text{or} \quad LogQ_t = LogQ_0 + \text{Kt}/2.303 \tag{8}$$

Q_t is the cumulative amount of drug released at time t, Q_0 is the initial amount of drug, K is the first order release constant, t is the time in hours.

Higuchi model was the first mathematical model aiming to describe drug release from a matrix system. Simplified Higuchi model relates the release of drugs to the square root of time based on Fickian diffusion equation[275, 359, 363]:

$$Q = K_H t^{1/2} \tag{9}$$

Q is the cumulative amount of drug released at time t, K_H is the Higuchi constant, t is the time in hours.

Korsmeyer-Peppas model was developed to specifically model the drug release from a polymeric system. It analyzes Fickian and non-Fickian diffusion of drug from swelling as well as non-swelling polymeric systems[364-368]. It is represented by equation (10):

$$\frac{M_t}{M_\infty} = \boldsymbol{K_{kp} t^n} \tag{10}$$

M_t/M_∞ is a fraction of drug released at time t, M_t is the amount of drug released in time t, M_∞ is the amount of drug released after time ∞, K_{kp} is the Korsmeyer release rate constant, t is the time in hours, n is the release exponent indicative of the mechanism of drug transport through the polymer. The n is estimated from linear regression of $\log\frac{M_t}{M_\infty}$ versus logt to characterize various release mechanisms. If n is less than 0.45, it means Quasi-Fickian diffusion. n=0.45 specifies Fickian diffusion and 0.45 < n < 0.89 specifies non-Fickian or anomalous diffusion. n=0.89 and above specify case-2 relaxation or super case transport-2. Non-Fickian or

anomalous diffusion is the diffusion-controlled release combined with the erosion-controlled release. Case-2 relaxation or super case transport-2 consists of the polymeric chain erosion, stresses and state-transition in hydrophilic glassy polymers swelling in water or biological fluids.

The BSA solution loaded DWMS with polymer mass ratios of 1:1 to1:3 have been fitted with Korsmeyer-Peppas kinetic. The values of n for them were < 0.45. The results indicated the drug released through Fickian diffusion from these DWMS. According to studies conducted by Shi *et al.*[357], Godbee, Weston and Mathiowitz [358], Yang, Chung and Ng[350], the presence of BSA solution resulted in more porous surface of DWMS. A small portion of drugs in the shell could directly diffuse through the surface pores. Moreover, the coalescence of BSA droplets within inner phase formed interconnecting water channels, inducing the drugs diffusing from core to shell. Nevertheless, the release models for BSA solid loaded DWMS were different. BSA solid loaded DWMS prepared with PLLA and PLGA mass ratio of 1:1 fitted with Higuchi kinetic, which means the release was controlled by Fickian diffusion. The R^2 of Korsmeyer-Peppas kinetic is relatively close to that of Higuchi kinetic and $n < 0.45$ demonstrated Quasi-Fickian diffusion. The diffusion contributed to a pretty low release of BSA which could be seen from Figure 15 because most of the drugs were in the core and only small amounts of BSA were on the shell surface diffusing from the microspheres. The model for BSA solid loaded DWMS with PLLA and PLGA mass ratio of 1:2 was Korsmeyer-Peppas and the value of n was between 0.45 and 0.89 demonstrating the release was because of the coaction of diffusion and erosion of the polymer. The drug was in the shell phase of DWMS in the polymer mass ratio of 1:2. Parts of the drug diffused from the shell to the exterior. In addition, the shell polymer PLGA has a faster degradation rate than the core polymer PLLA. Therefore, the degradation of shell improved the BSA release from shell phase. The BSA solid loaded DWMS with PLLA and PLGA mass ratio of 1:3 has been fitted with Higuchi model showing

the release was controlled by Fickian diffusion. Since the R^2 of Higuchi model is relatively close to the R^2 of Korsmeyer-Peppas kinetic, we also used Korsmeyer-Peppas kinetic to analyse the release. The value of n was between 0.45 and 0.89 demonstrating the release was also controlled by anomalous diffusion. To sum up, the release was due to primarily Fickian diffusion and anomalous diffusion as a subsidiary. Same as polymer mass ratio of 1:2, the drug was located in the shell and the shell material PLGA degrades faster than core material PLLA, resulting in diffusion of drug and erosion of PLGA. However, the shell material became thicker when the PLLA and PLGA mass ratio was 1:3. This slowed down the erosion of the PLGA polymer, thus leading to the erosion of polymer to be less impactful.

Table 8. Result of drug release mechanism of BSA loaded DWMS

Formulation	Zero order (R^2)	First order (R^2)	Higuchi (R^2)	Korsmeyer-Peppas (R^2)	Korsmeyer-Peppas (n)	Drug transport mechanisms
1:1 BSA solid loaded DWMS	0.8360	0.8387	0.9220	0.8820	0.4438	Fickian diffusion
1:2 BSA solid loaded DWMS	0.5581	0.5757	0.7658	0.8636	0.5971	Anomalous diffusion
1:3 BSA solid loaded DWMS	0.6115	0.6321	0.7920	0.7555	0.8861	Primary Fickian diffusion and anomalous diffusion as subsidiary
1:1 BSA solution loaded DWMS	0.4705	0.5219	0.6899	0.8387	0.3968	Fickian diffusion
1:2 BSA solution loaded DWMS	0.6807	0.7738	0.8657	0.9463	0.3319	Fickian diffusion
1:3 BSA solution loaded DWMS	0.7804	0.8757	0.9344	0.9785	0.391	Fickian diffusion

5. Conclusions and future work

In this study, we determined if the double-walled polymeric microsphere could be a drug delivery system with a well-sustained release profile that can be implanted during DC

procedure as a potential stroke treatment. First, the fabrication parameters of DWMS were optimized resulting in high yields and desirable formations. DWMS comprising of a shell that limited the drug release rate and a core encapsulated with drug, was successfully produced applying a solvent evaporation technique utilizing phase separation. Furthermore, studies that examined the PLLA and PLGA polymer mass ratio causing core-shell reversion enabled us to entrap hydrophilic drug within the inner core of DWMS. The characterizations of DWMS were also performed to allow for accurate identification of the shell and core compositions in different polymer mass ratios and preferential distribution of BSA in different forms in two polymer layers. In addition, the drug delivery system designed for this thesis achieved high encapsulation efficiency for a hydrophilic drug accompanied by release profiles containing a time lag phase and potential sustained release with low initial burst. This confirmed DWMS is feasible to be a potential sustainable drug delivering and releasing system to load growth factors to stimulate endogenous regeneration.

Though the results of the above experiments are interesting, several further studies still need to be completed. The first one is the development of further controlling the size of DWMS. The large size of the DWMS is an obstacle to administrate intravenous injection, which necessitates surgical operations. According to Lee *et al.*[369], increasing mechanical stirring speed from 350rpm to 2000rpm and PVA concentration from 0.5% w/v to 6% w/v reduced particle sizes from 276 ± 58.5 μm to approximately 18.3 ± 4.8μm. Moreover, the organic solvent evaporation rate affects the particle mean diameters and size distribution. Mainardes and Evangelista presented that using a vacuum rotative evaporator resulted in particle diameters of 298±35 μm, which was smaller than that obtained from magnetic stirring under normal pressure with diameters of 390±27 μm[370]. This is due to the shorter solvent evaporation time with the aid of reduced pressure, which causes higher diffusion rate of the organic solvent through the interface[370]. In addition, increased microsphere size was found

due to decreasing BSA liquid emulsion droplet size in the W/O/W system and increasing BSA powder size in the S/O/W system by Maa and Hsu[354]. The second matter is the studies of growth factors encapsulated into DWMS. In our current study, BSA was used as a model protein to be loaded in DWMS. For future steps, the release profiles of growth factors will be performed to further verify the feasibility of DWMS as a drug delivery system for sustained release. The third is the incorporation of drug-loaded DWMS into BC duraplasty to create a composite drug delivering and releasing system. Currently, growth factors loaded directly onto the BC duraplasty can only achieve sustained release for less than 14 days[34]. To achieve more controllable drug releases, DWMS combining with BC duraplasty can act as a composite drug system to load and release more than one therapeutic molecule during different time periods.

6. Reference

1. Bang, O.Y., et al., *Adult Stem Cell Therapy for Stroke: Challenges and Progress.* J Stroke, 2016. 18(3): p. 256-266.
2. Gratz, P.P., et al., *Outcome of standard and high-risk patients with acute anterior circulation stroke after stent retriever thrombectomy.* Stroke, 2014. 45(1): p. 152-8.
3. Donkor, E.S., *Stroke in the 21(st) Century: A Snapshot of the Burden, Epidemiology, and Quality of Life.* Stroke Res Treat, 2018. 2018: p. 3238165.
4. Upadhyay, R.K., *Drug delivery systems, CNS protection, and the blood brain barrier.* Biomed Res Int, 2014. 2014: p. 869269.
5. Hawkins, B.T. and T.P. Davis, *The blood-brain barrier/neurovascular unit in health and disease.* Pharmacol Rev, 2005. 57(2): p. 173-85.
6. Gabathuler, R., *Approaches to transport therapeutic drugs across the blood-brain barrier to treat brain diseases.* Neurobiol Dis, 2010. 37(1): p. 48-57.
7. Fernandes, L.F., et al., *Recent Advances in the Therapeutic and Diagnostic Use of Liposomes and Carbon Nanomaterials in Ischemic Stroke.* Front Neurosci, 2018. 12: p. 453.
8. Baker, E.W., H.A. Kinder, and F.D. West, *Neural stem cell therapy for stroke: A multimechanistic approach to restoring neurological function.* Brain Behav, 2019. 9(3): p. e01214.
9. Bhaskar, S., et al., *Reperfusion therapy in acute ischemic stroke: dawn of a new era?* BMC Neurology, 2018. 18(1): p. 8.
10. Krause, M., et al., *Cell-Based Therapies for Stroke: Are We There Yet?* Frontiers in Neurology, 2019. 10(656).
11. Nogueira, R.G., et al., *Thrombectomy 6 to 24 Hours after Stroke with a Mismatch between Deficit and Infarct.* New England Journal of Medicine, 2017. 378(1): p. 11-21.
12. Catanese, L., J. Tarsia, and M. Fisher, *Acute Ischemic Stroke Therapy Overview.* Circulation Research, 2017. 120(3): p. 541-558.
13. Beckhauser, M.T., et al., *Extended Time Window Mechanical Thrombectomy for Acute Stroke in Brazil.* Journal of Stroke and Cerebrovascular Diseases, 2020. 29(10): p. 105134.
14. Yoo, A.J. and T. Andersson, *Thrombectomy in Acute Ischemic Stroke: Challenges to Procedural Success.* Journal of stroke, 2017. 19(2): p. 121-130.
15. Chamorro, Á., et al., *Neuroprotection in acute stroke: targeting excitotoxicity, oxidative and nitrosative stress, and inflammation.* Lancet Neurol, 2016. 15(8): p. 869-881.
16. Thomalla, G., et al., *MRI-Guided Thrombolysis for Stroke with Unknown Time of Onset.* The New England journal of medicine, 2018. 379.
17. Grefkes, C. and G.R. Fink, *Recovery from stroke: current concepts and future perspectives.* Neurological Research and Practice, 2020. 2(1): p. 17.
18. Burns, T.C., C.M. Verfaillie, and W.C. Low, *Stem cells for ischemic brain injury: a critical review.* J Comp Neurol, 2009. 515(1): p. 125-44.
19. Fagan, S.C., et al., *Recommendations for preclinical research in hemorrhagic transformation.* Transl Stroke Res, 2013. 4(3): p. 322-7.
20. Mayer, S.A. and F. Rincon, *Treatment of intracerebral haemorrhage.* Lancet Neurol, 2005. 4(10): p. 662-72.
21. Banerjee, S., et al., *The potential benefit of stem cell therapy after stroke: an update.* Vasc Health Risk Manag, 2012. 8: p. 569-80.
22. Buja, L.M. and D. Vela, *Immunologic and inflammatory reactions to exogenous stem cells implications for experimental studies and clinical trials for myocardial repair.* J Am Coll Cardiol, 2010. 56(21): p. 1693-700.
23. Xu, W., et al., *Neuroprotective Effects of Stem Cells in Ischemic Stroke.* Stem Cells Int, 2017. 2017: p. 4653936.

24. Kaneko, N., E. Kako, and K. Sawamoto, *Prospects and limitations of using endogenous neural stem cells for brain regeneration.* Genes (Basel), 2011. 2(1): p. 107-30.
25. Arvidsson, A., et al., *Neuronal replacement from endogenous precursors in the adult brain after stroke.* Nat Med, 2002. 8(9): p. 963-70.
26. Lanfranconi, S., et al., *Growth factors in ischemic stroke.* J Cell Mol Med, 2011. 15(8): p. 1645-87.
27. Moshayedi, P., et al., *Systematic optimization of an engineered hydrogel allows for selective control of human neural stem cell survival and differentiation after transplantation in the stroke brain.* Biomaterials, 2016. 105: p. 145-155.
28. Kaplan, M.S. and D.H. Bell, *Mitotic neuroblasts in the 9-day-old and 11-month-old rodent hippocampus.* J Neurosci, 1984. 4(6): p. 1429-41.
29. Alvarez-Buylla, A. and J.M. Garcı´a-Verdugo, *Neurogenesis in Adult Subventricular Zone.* The Journal of Neuroscience, 2002. 22(3): p. 629.
30. Sanai, N., et al., *Unique astrocyte ribbon in adult human brain contains neural stem cells but lacks chain migration.* Nature, 2004. 427(6976): p. 740-4.
31. Curtis, M.A., P.S. Eriksson, and R.L. Faull, *Progenitor cells and adult neurogenesis in neurodegenerative diseases and injuries of the basal ganglia.* Clin Exp Pharmacol Physiol, 2007. 34(5-6): p. 528-32.
32. Eghwrudjakpor, P.O. and A.B. Allison, *Decompressive craniectomy following brain injury: factors important to patient outcome.* Libyan J Med, 2010. 5.
33. Beez, T., et al., *Decompressive craniectomy for acute ischemic stroke.* Critical Care, 2019. 23(1): p. 209.
34. Stumpf, T.R., et al., *Design and evaluation of a biosynthesized cellulose drug releasing duraplasty.* Mater Sci Eng C Mater Biol Appl, 2020. 110: p. 110677.
35. Kelmendi-Doko, A., et al., *Controlled dexamethasone delivery via double-walled microspheres to enhance long-term adipose tissue retention.* J Tissue Eng, 2017. 8: p. 2041731417735402.
36. Han, F.Y., et al., *Bioerodable PLGA-Based Microparticles for Producing Sustained-Release Drug Formulations and Strategies for Improving Drug Loading.* Front Pharmacol, 2016. 7: p. 185.
37. Brannon-Peppas, L., *Recent advances on the use of biodegradable microparticles and nanoparticles in controlled drug delivery.* International Journal of Pharmaceutics, 1995. 116(1): p. 1-9.
38. Santhosh, K.T., A. Alizadeh, and S. Karimi-Abdolrezaee, *Design and optimization of PLGA microparticles for controlled and local delivery of Neuregulin-1 in traumatic spinal cord injury.* J Control Release, 2017. 261: p. 147-162.
39. Wang, W., et al., *Fabrication and evaluation of nanoparticle-assembled BSA microparticles for enhanced liver delivery of glycyrrhetinic acid.* Artif Cells Nanomed Biotechnol, 2017. 45(4): p. 740-747.
40. Xia, Y., et al., *Protein encapsulation in and release from monodisperse double-wall polymer microspheres.* J Pharm Sci, 2013. 102(5): p. 1601-9.
41. Tan, E.C., R. Lin, and C.H. Wang, *Fabrication of double-walled microspheres for the sustained release of doxorubicin.* J Colloid Interface Sci, 2005. 291(1): p. 135-43.
42. Tan, H. and J. Ye, *Surface morphology and in vitro release performance of double-walled PLLA/PLGA microspheres entrapping a highly water-soluble drug.* Applied Surface Science, 2008. 255(2): p. 353-356.
43. Kokai, L., et al., *Protein bioactivity and polymer orientation is affected by stabilizer incorporation for double-walled microspheres.* Journal of controlled release : official journal of the Controlled Release Society, 2009. 141: p. 168-76.
44. Katan, M. and A. Luft, *Global Burden of Stroke.* Semin Neurol, 2018. 38(2): p. 208-211.
45. *World Health Organization, "Stroke, Cerebrovascular accident," 2020. [Online].* Available from: http://www.emro.who.int/health-topics/stroke-cerebrovascular-accident/index.html.

46. *Government of Canada, "Stroke in Canada: Highlights from the Canadian Chronic Disease Surveillance System," 2020. [Online].* Available from: https://www.canada.ca/en/public-health/services/publications/diseases-conditions/stroke-canada-fact-sheet.html.
47. *Canadian Healthcare Technology, "Tele-rehab found to be effective for stroke patients," 2019. [Online].* Available from: https://www.canhealth.com/2019/10/08/tele-rehab-found-to-be-effective-for-stroke-patients/.
48. Dirnagl, U., C. Iadecola, and M.A. Moskowitz, *Pathobiology of ischaemic stroke: an integrated view.* Trends in Neurosciences, 1999. 22(9): p. 391-397.
49. Allen, C.L. and U. Bayraktutan, *Risk Factors for Ischaemic Stroke.* International Journal of Stroke, 2008. 3(2): p. 105-116.
50. Sudharani, K., T.C. Sarma, and K.S. Prasad. *Brain stroke detection using K-Nearest Neighbor and Minimum Mean Distance technique*. in *2015 International Conference on Control, Instrumentation, Communication and Computational Technologies (ICCICCT)*. 2015.
51. Sutherland, G.R. and R.N. Auer, *Primary intracerebral hemorrhage.* Journal of Clinical Neuroscience, 2006. 13(5): p. 511-517.
52. Hankey, G.J., *Management of the first-time transient ischaemic attack.* Emergency Medicine, 2001. 13(1): p. 70-81.
53. Swan, J., J.M. Jouria Jr, and M.J. Katz, *Stroke: Comprehensive Acute Stroke Care.* 2016.
54. Jivan, K., K. Ranchod, and G. Modi, *Management of ischaemic stroke in the acute setting: review of the current status.* Cardiovasc J Afr, 2013. 24(3): p. 86-92.
55. Fisher, M. and G.W. Albers, *Advanced imaging to extend the therapeutic time window of acute ischemic stroke.* Ann Neurol, 2013. 73(1): p. 4-9.
56. Fonarow, G.C., et al., *Timeliness of tissue-type plasminogen activator therapy in acute ischemic stroke: patient characteristics, hospital factors, and outcomes associated with door-to-needle times within 60 minutes.* Circulation, 2011. 123(7): p. 750-8.
57. Lees, K.R., et al., *Time to treatment with intravenous alteplase and outcome in stroke: an updated pooled analysis of ECASS, ATLANTIS, NINDS, and EPITHET trials.* Lancet, 2010. 375(9727): p. 1695-703.
58. Gravanis, I. and S.E. Tsirka, *Tissue-type plasminogen activator as a therapeutic target in stroke.* Expert Opin Ther Targets, 2008. 12(2): p. 159-70.
59. Peña, I.d., et al., *Strategies to Extend Thrombolytic Time Window for Ischemic Stroke Treatment: An Unmet Clinical Need.* J Stroke, 2017. 19(1): p. 50-60.
60. Zivin, J.A., *Factors determining the therapeutic window for stroke.* Neurology, 1998. 50(3): p. 599.
61. Sharma, V.K., et al., *Recanalization Therapies in Acute Ischemic Stroke: Pharmacological Agents, Devices, and Combinations.* Stroke Research and Treatment, 2010. 2010: p. 672064.
62. Jin, R., et al., *Taurine Reduces tPA (Tissue-Type Plasminogen Activator)-Induced Hemorrhage and Microvascular Thrombosis After Embolic Stroke in Rat.* Stroke, 2018. 49: p. STROKEAHA.118.020747.
63. Docagne, F., et al., *Understanding the Functions of Endogenous and Exogenous Tissue-Type Plasminogen Activator During Stroke.* Stroke, 2015. 46(1): p. 314-320.
64. Fredriksson, L., D.A. Lawrence, and R.L. Medcalf, *tPA Modulation of the Blood-Brain Barrier: A Unifying Explanation for the Pleiotropic Effects of tPA in the CNS.* Semin Thromb Hemost, 2017. 43(2): p. 154-168.
65. Kaur, J., et al., *The Neurotoxicity of Tissue Plasminogen Activator?* Journal of Cerebral Blood Flow & Metabolism, 2004. 24(9): p. 945-963.
66. Whiteley, W.N., et al., *Risk Factors for Intracranial Hemorrhage in Acute Ischemic Stroke Patients Treated With Recombinant Tissue Plasminogen Activator.* Stroke, 2012. 43(11): p. 2904-2909.
67. Marinkovic, I., et al., *Evolution of Intracerebral Hemorrhage after Intravenous Tpa: Reversal of Harmful Effects with Mast Cell Stabilization.* Journal of Cerebral Blood Flow & Metabolism, 2014. 34(1): p. 176-181.

68. Law, L.Y., B.C.V. Campbell, and T. Wijeratne, *Advances in endovascular therapy for ischemic stroke: A whole new ball game.* Neurol Clin Pract, 2016. 6(1): p. 49-54.
69. Phipps, M.S. and C.A. Cronin, *Management of acute ischemic stroke.* BMJ, 2020. 368: p. l6983.
70. Sacks, D., et al., *Multisociety Consensus Quality Improvement Guidelines for Intraarterial Catheter-directed Treatment of Acute Ischemic Stroke, from the American Society of Neuroradiology, Canadian Interventional Radiology Association, Cardiovascular and Interventional Radiological Society of Europe, Society for Cardiovascular Angiography and Interventions, Society of Interventional Radiology, Society of NeuroInterventional Surgery, European Society of Minimally Invasive Neurological Therapy, and Society of Vascular and Interventional Neurology.* AJNR Am J Neuroradiol, 2013. 34(4): p. E0.
71. Snelling, B., et al., *Extended Window for Stroke Thrombectomy.* Journal of neurosciences in rural practice, 2019. 10(2): p. 294-300.
72. Salam, S., et al., *E-098 Mechanical thrombectomy in the extended 24 hour time window for acute ischemic stroke patients with large vessel occlusion*. Vol. 12. 2020. A82.2-A82.
73. Harrichandparsad, R., *Mechanical thrombectomy for acute ischaemic stroke*. 2019. Vol. 109. 2019.
74. Goldhoorn, R.-J.B., et al., *Safety and Outcome of Endovascular Treatment in Prestroke-Dependent Patients*. Stroke, 2018. 49(10): p. 2406-2414.
75. Meinel, T.R., et al., *Endovascular Stroke Treatment and Risk of Intracranial Hemorrhage in Anticoagulated Patients.* Stroke, 2020. 51(3): p. 892-898.
76. Josephson, S.A. and H. Kamel, *The Acute Stroke Care Revolution: Enhancing Access to Therapeutic Advances*. Jama, 2018. 320(12): p. 1239-1240.
77. Wang, H.Y., et al., *Outcomes of microsurgical clipping vs coil embolization for ruptured aneurysmal subarachnoid hemorrhage: A multicenter real-world analysis of 583 patients in China.* Medicine (Baltimore), 2019. 98(33): p. e16821.
78. *Coil embolization for intracranial aneurysms: an evidence-based analysis*. Ont Health Technol Assess Ser, 2006. 6(1): p. 1-114.
79. de Oliveira Manoel, A.L., *Surgery for spontaneous intracerebral hemorrhage.* Crit Care, 2020. 24(1): p. 45.
80. Kitago, T. and R.R. Ratan, *Rehabilitation following hemorrhagic stroke: building the case for stroke-subtype specific recovery therapies*. F1000Res, 2017. 6: p. 2044.
81. Gaciong, Z., M. Siński, and J. Lewandowski, *Blood pressure control and primary prevention of stroke: summary of the recent clinical trial data and meta-analyses.* Curr Hypertens Rep, 2013. 15(6): p. 559-74.
82. Borlongan, C.V., *Concise Review: Stem Cell Therapy for Stroke Patients: Are We There Yet?* Stem Cells Transl Med, 2019. 8(9): p. 983-988.
83. Biehl, J.K. and B. Russell, *Introduction to stem cell therapy.* J Cardiovasc Nurs, 2009. 24(2): p. 98-103; quiz 104-5.
84. Zakrzewski, W., et al., *Stem cells: past, present, and future*. Stem Cell Research & Therapy, 2019. 10(1): p. 68.
85. Reubinoff, B.E., et al., *Embryonic stem cell lines from human blastocysts: somatic differentiation in vitro.* Nature Biotechnology, 2000. 18(4): p. 399-404.
86. Haas, S., N. Weidner, and J. Winkler, *Adult stem cell therapy in stroke.* Curr Opin Neurol, 2005. 18(1): p. 59-64.
87. Meyers, P.M., et al., *Current Status of Endovascular Stroke Treatment.* Circulation, 2011. 123(22): p. 2591-2601.
88. Kelly, S., et al., *Transplanted human fetal neural stem cells survive, migrate, and differentiate in ischemic rat cerebral cortex.* Proc Natl Acad Sci U S A, 2004. 101(32): p. 11839-44.
89. Mattsson, B., et al., *Neural grafting to experimental neocortical infarcts improves behavioral outcome and reduces thalamic atrophy in rats housed in enriched but not in standard environments*. Stroke, 1997. 28(6): p. 1225-31; discussion 1231-2.

90. Nishino, H. and C.V. Borlongan, *Restoration of function by neural transplantation in the ischemic brain.* Prog Brain Res, 2000. 127: p. 461-76.
91. Glover, J., *Can We Use Human Embryonic Stem Cells to Treat Brain and Spinal Cord Injury and Disease?* 2008. p. 55-70.
92. Marei, H.E., et al., *Potential of Stem Cell-Based Therapy for Ischemic Stroke.* Front Neurol, 2018. 9: p. 34.
93. Janowski, M., D.-C. Wagner, and J. Boltze, *Stem Cell–Based Tissue Replacement After Stroke.* Stroke, 2015. 46(8): p. 2354-2363.
94. Napoli, E. and C.V. Borlongan, *Recent Advances in Stem Cell-Based Therapeutics for Stroke.* Transl Stroke Res, 2016. 7(6): p. 452-457.
95. Boese, A.C., et al., *Neural stem cell therapy for subacute and chronic ischemic stroke.* Stem Cell Research & Therapy, 2018. 9(1): p. 154.
96. Barkho, B.Z. and X. Zhao, *Adult neural stem cells: response to stroke injury and potential for therapeutic applications.* Curr Stem Cell Res Ther, 2011. 6(4): p. 327-38.
97. Ding, D.-C., et al., *Current Concepts in Adult Stem Cell Therapy for Stroke.* Current medicinal chemistry, 2006. 13: p. 3565-74.
98. Naoko, K., E. Kako, and K. Sawamoto, *Prospects and Limitations of Using Endogenous Neural Stem Cells for Brain Regeneration.* Genes, 2011. 2: p. 107-30.
99. Martínez-Morales, P.L., et al., *Progress in Stem Cell Therapy for Major Human Neurological Disorders.* Stem Cell Reviews and Reports, 2013. 9(5): p. 685-699.
100. Chen, J., et al., *Therapeutic benefit of intracerebral transplantation of bone marrow stromal cells after cerebral ischemia in rats.* J Neurol Sci, 2001. 189(1-2): p. 49-57.
101. Zhang, Z.G., et al., *Magnetic resonance imaging and neurosphere therapy of stroke in rat.* Ann Neurol, 2003. 53(2): p. 259-63.
102. Taguchi, A., et al., *Administration of CD34+ cells after stroke enhances neurogenesis via angiogenesis in a mouse model.* J Clin Invest, 2004. 114(3): p. 330-8.
103. Shyu, W.C., et al., *Intracerebral peripheral blood stem cell (CD34+) implantation induces neuroplasticity by enhancing beta1 integrin-mediated angiogenesis in chronic stroke rats.* J Neurosci, 2006. 26(13): p. 3444-53.
104. Bao, X.J., et al., *Transplantation of Flk-1+ human bone marrow-derived mesenchymal stem cells promotes behavioral recovery and anti-inflammatory and angiogenesis effects in an intracerebral hemorrhage rat model.* Int J Mol Med, 2013. 31(5): p. 1087-96.
105. Sun, Q., Z. Zhang, and Z. Sun, *The potential and challenges of using stem cells for cardiovascular repair and regeneration.* Genes Dis, 2014. 1(1): p. 113-119.
106. Binato, R., et al., *Stability of human mesenchymal stem cells during in vitro culture: Considerations for cell therapy.* Cell proliferation, 2012. 46.
107. Kawai, H., et al., *Tridermal tumorigenesis of induced pluripotent stem cells transplanted in ischemic brain.* J Cereb Blood Flow Metab, 2010. 30(8): p. 1487-93.
108. Huang, L. and L. Zhang, *Neural stem cell therapies and hypoxic-ischemic brain injury.* Prog Neurobiol, 2019. 173: p. 1-17.
109. Uzun, G., D. Subhani, and S. Amor, *Trophic factors and stem cells for promoting recovery in stroke.* J Vasc Interv Neurol, 2010. 3(1): p. 3-12.
110. Younsi, A., et al., *Three Growth Factors Induce Proliferation and Differentiation of Neural Precursor Cells In Vitro and Support Cell-Transplantation after Spinal Cord Injury In Vivo.* Stem Cells International, 2020. 2020: p. 5674921.
111. Gustafsson, E., et al., *Anterograde delivery of brain-derived neurotrophic factor to striatum via nigral transduction of recombinant adeno-associated virus increases neuronal death but promotes neurogenic response following stroke.* Eur J Neurosci, 2003. 17(12): p. 2667-78.
112. Chmielnicki, E., et al., *Adenovirally expressed noggin and brain-derived neurotrophic factor cooperate to induce new medium spiny neurons from resident progenitor cells in the adult striatal ventricular zone.* J Neurosci, 2004. 24(9): p. 2133-42.

113. Schänzer, A., et al., *Direct stimulation of adult neural stem cells in vitro and neurogenesis in vivo by vascular endothelial growth factor.* Brain Pathol, 2004. 14(3): p. 237-48.
114. Jin, K., et al., *Vascular endothelial growth factor (VEGF) stimulates neurogenesis in vitro and in vivo.* Proc Natl Acad Sci U S A, 2002. 99(18): p. 11946-50.
115. Zhu, W., et al., *Intranasal nerve growth factor enhances striatal neurogenesis in adult rats with focal cerebral ischemia.* Drug Deliv, 2011. 18(5): p. 338-43.
116. Gudasheva, T.A., et al., *A Nerve Growth Factor Dipeptide Mimetic Stimulates Neurogenesis and Synaptogenesis in the Hippocampus and Striatum of Adult Rats with Focal Cerebral Ischemia.* Acta Naturae, 2019. 11(3): p. 31-37.
117. Kuhn, H.G., et al., *Epidermal growth factor and fibroblast growth factor-2 have different effects on neural progenitors in the adult rat brain.* J Neurosci, 1997. 17(15): p. 5820-9.
118. Teramoto, T., et al., *EGF amplifies the replacement of parvalbumin-expressing striatal interneurons after ischemia.* J Clin Invest, 2003. 111(8): p. 1125-32.
119. Yoshimura, S., et al., *FGF-2 regulation of neurogenesis in adult hippocampus after brain injury.* Proceedings of the National Academy of Sciences of the United States of America, 2001. 98: p. 5874-9.
120. Woodbury, M.E. and T. Ikezu, *Fibroblast growth factor-2 signaling in neurogenesis and neurodegeneration.* J Neuroimmune Pharmacol, 2014. 9(2): p. 92-101.
121. Cheng, X., et al., *Acidic fibroblast growth factor delivered intranasally induces neurogenesis and angiogenesis in rats after ischemic stroke.* Neurol Res, 2011. 33(7): p. 675-80.
122. Sugimori, H., H. Speller, and S. Finklestein, *Intravenous basic fibroblast growth factor produces a persistent reduction in infarct volume following permanent focal ischemia in rats.* Neuroscience letters, 2001. 300: p. 13-6.
123. Ninomiya, M., et al., *Enhanced neurogenesis in the ischemic striatum following EGF-induced expansion of transit-amplifying cells in the subventricular zone.* Neurosci Lett, 2006. 403(1-2): p. 63-7.
124. Greenberg, D.A. and K. Jin, *Vascular endothelial growth factors (VEGFs) and stroke.* Cell Mol Life Sci, 2013. 70(10): p. 1753-61.
125. Sun, Y., et al., *VEGF-induced neuroprotection, neurogenesis, and angiogenesis after focal cerebral ischemia.* J Clin Invest, 2003. 111(12): p. 1843-51.
126. Li, X., et al., *Intranasal administration of nerve growth factor promotes angiogenesis via activation of PI3K/Akt signaling following cerebral infarction in rats.* Am J Transl Res, 2018. 10(11): p. 3481-3492.
127. Schäbitz, W.R., et al., *Intravenous brain-derived neurotrophic factor enhances poststroke sensorimotor recovery and stimulates neurogenesis.* Stroke, 2007. 38(7): p. 2165-72.
128. Schäbitz, W.R., et al., *Intraventricular brain-derived neurotrophic factor reduces infarct size after focal cerebral ischemia in rats.* J Cereb Blood Flow Metab, 1997. 17(5): p. 500-6.
129. Li, R., et al., *Growth factors-based therapeutic strategies and their underlying signaling mechanisms for peripheral nerve regeneration.* Acta Pharmacologica Sinica, 2020. 41(10): p. 1289-1300.
130. Hu, F., et al., *Effects of epidermal growth factor and basic fibroblast growth factor on the proliferation and osteogenic and neural differentiation of adipose-derived stem cells.* Cell Reprogram, 2013. 15(3): p. 224-32.
131. Sun, X.-T., et al., *Angiogenic synergistic effect of basic fibroblast growth factor and vascular endothelial growth factor in an in vitro quantitative microcarrier-based three-dimensional fibrin angiogenesis system.* World journal of gastroenterology, 2004. 10(17): p. 2524-2528.
132. Asahara, T., et al., *Synergistic effect of vascular endothelial growth factor and basic fibroblast growth factor on angiogenesis in vivo.* Circulation, 1995. 92(9 Suppl): p. Ii365-71.
133. Almodovar, C.R.d., et al., *Role and Therapeutic Potential of VEGF in the Nervous System.* Physiological Reviews, 2009. 89(2): p. 607-648.

134. Friden, P.M., et al., *Blood-brain barrier penetration and in vivo activity of an NGF conjugate.* Science, 1993. 259(5093): p. 373-7.
135. Yi, X., et al., *Agile delivery of protein therapeutics to CNS.* J Control Release, 2014. 190: p. 637-63.
136. Hersh, D.S., et al., *Evolving Drug Delivery Strategies to Overcome the Blood Brain Barrier.* Current pharmaceutical design, 2016. 22(9): p. 1177-1193.
137. Garg, T., et al., *Current strategies for targeted delivery of bio-active drug molecules in the treatment of brain tumor.* Journal of drug targeting, 2015. 23: p. 1-23.
138. Kim, H.-K., et al., *Intracerebroventricular Administration of Fibroblast Growth Factor Receptor Inhibitor Attenuates High-Phosphate Diet-Induced Exercise Pressor Reflex Overactivation in Rats.* The FASEB Journal, 2019. 33(S1): p. 540.4-540.4.
139. Pan, W., et al., *Permeation of hepatocyte growth factor across the blood-brain barrier.* Exp Neurol, 2006. 201(1): p. 99-104.
140. Greenberg, D.A. and K. Jin, *Growth factors and stroke.* NeuroRx, 2006. 3(4): p. 458-65.
141. Lindvall, O. and Z. Kokaia, *Neurogenesis following Stroke Affecting the Adult Brain.* Cold Spring Harb Perspect Biol, 2015. 7(11).
142. Nih, L.R., et al., *Injection of Microporous Annealing Particle (MAP) Hydrogels in the Stroke Cavity Reduces Gliosis and Inflammation and Promotes NPC Migration to the Lesion.* Adv Mater, 2017. 29(32).
143. Love, C.J., et al., *Biomaterials for Stroke Therapy.* Stroke, 2019. 50(8): p. 2278-2284.
144. Shah, S. and W.T. Kimberly, *Today's Approach to Treating Brain Swelling in the Neuro Intensive Care Unit.* Semin Neurol, 2016. 36(6): p. 502-507.
145. Appelboom, G., et al., *Aquaporin-4 gene variant independently associated with oedema after intracerebral haemorrhage.* Neurol Res, 2015. 37(8): p. 657-61.
146. Pallesen, L.P., K. Barlinn, and V. Puetz, *Role of Decompressive Craniectomy in Ischemic Stroke.* Front Neurol, 2018. 9: p. 1119.
147. Kurland, D.B., et al., *Complications Associated with Decompressive Craniectomy: A Systematic Review.* Neurocrit Care, 2015. 23(2): p. 292-304.
148. Gopalakrishnan, M., et al., *Complications of decompressive craniectomy.* Frontiers in neurology, 2018. 9: p. 977.
149. Wang, R., et al., *Outcomes of Early Decompressive Craniectomy Versus Conventional Medical Management After Severe Traumatic Brain Injury: A Systematic Review and Meta-Analysis.* Medicine, 2015. 94(43): p. e1733-e1733.
150. Rubiano, A.M., et al., *The Role of Decompressive Craniectomy in the Context of Severe Traumatic Brain Injury: Summary of Results and Analysis of the Confidence Level of Conclusions From Systematic Reviews and Meta-Analyses.* Frontiers in neurology, 2019. 10: p. 1063-1063.
151. Kamal Alam, B., et al., *Functional Outcome After Decompressive Craniectomy in Patients with Dominant or Non-Dominant Malignant Middle Cerebral Infarcts.* Cureus, 2017. 9(1): p. e997.
152. *Purves D, Augustine GJ, Fitzpatrick D, et al., editors. Neuroscience. 2nd edition. Sunderland (MA): Sinauer Associates; 2001. The Meninges. Available from: https://www.ncbi.nlm.nih.gov/books/NBK10877/.*
153. *Ghannam JY, Al Kharazi KA. Neuroanatomy, Cranial Meninges. [Updated 2020 Jul 31]. In: StatPearls [Internet]. Treasure Island (FL): StatPearls Publishing; 2020 Jan-. Available from: https://www.ncbi.nlm.nih.gov/books/NBK539882/.*
154. Kerber, K.A., *Fundamental Neuroscience for Basic and Clinical Applications, 3rd Edition.* Journal of Neuro-Ophthalmology, 2008. 28(4): p. 365-366.
155. Jacob, S., *Chapter 7 - Head and neck*, in *Human Anatomy*, S. Jacob, Editor. 2008, Churchill Livingstone. p. 181-225.
156. Liddelow, S.A., *Fluids and barriers of the CNS: a historical viewpoint.* Fluids and Barriers of the CNS, 2011. 8(1): p. 2.

157. *"LibreTexts libraries," [Online]. Available: https://bio.libretexts.org/@api/deki/files/9182/OSC_Microbio_26_01_Meninges.jpg?revision=1*.
158. Masang Ban Bolly, H., et al., *The ideal selection criteria for duraplasty material in brain surgery: A review.* Interdisciplinary Neurosurgery, 2020. 22: p. 100800.
159. Berjano, R., F.C. Vinas, and M. Dujovny, *A review of dural substitutes used in neurosurgery.* Critical Reviews in Neurosurgery, 1999. 9(4): p. 217-222.
160. Turchan, A., et al., *Duraplasty using amniotic membrane versus temporal muscle fascia: A clinical comparative study.* J Clin Neurosci, 2018. 50: p. 272-276.
161. Barbolt, T.A., et al., *Biocompatibility evaluation of dura mater substitutes in an animal model.* Neurol Res, 2001. 23(8): p. 813-20.
162. Velnar, T. and L. Gradisnik, *Soft tissue grafts for dural reconstruction after meningioma surgery.* Bosnian journal of basic medical sciences, 2019. 19(3): p. 297-303.
163. Abuzayed, B., et al., *Duraplasty using autologous fascia lata reenforced by on-site pedicled muscle flap: technical note.* J Craniofac Surg, 2009. 20(2): p. 435-8.
164. Laun, A., J.C. Tonn, and C. Jerusalem, *Comparative study of lyophilized human dura mater and lyophilized bovine pericardium as dural substitutes in neurosurgery.* Acta Neurochir (Wien), 1990. 107(1-2): p. 16-21.
165. Wang, H.T., et al., *Free flap reconstruction of the scalp and calvaria of major neurosurgical resections in cancer patients: lessons learned closing large, difficult wounds of the dura and skull.* Plast Reconstr Surg, 2007. 119(3): p. 865-72.
166. Dufrane, D., et al., *Clinical application of a physically and chemically processed human substitute for dura mater.* J Neurosurg, 2003. 98(6): p. 1198-202.
167. Alleyne, C.H., Jr. and D.L. Barrow, *Immune response in hosts with cadaveric dural grafts. Report of two cases.* J Neurosurg, 1994. 81(4): p. 610-3.
168. al Fauzi, A., A. Paramadini, and T. Fatchur Rochman, *Clinical Trial and Preparation of Amniotic Membrane as Dura Mater Artificial*. 2017. 18-20.
169. Yamada, K., et al., *Development of a dural substitute from synthetic bioabsorbable polymers.* J Neurosurg, 1997. 86(6): p. 1012-7.
170. Yamada, K., et al., *Clinical application of a new bioabsorbable artificial dura mater.* J Neurosurg, 2002. 96(4): p. 731-5.
171. Parízek, J., et al., *Xenogeneic pericardium as a dural substitute in reconstruction of suboccipital dura mater in children.* J Neurosurg, 1989. 70(6): p. 905-9.
172. Xu, B.Z., et al., *Study and clinical application of a porcine biomembrane for the repair of dural defects.* J Neurosurg, 1988. 69(5): p. 707-11.
173. O'Neill, P. and A.E. Booth, *Use of porcine dermis as a dural substitute in 72 patients.* J Neurosurg, 1984. 61(2): p. 351-4.
174. Gazzeri, R., et al., *Transparent equine collagen biomatrix as dural repair. A prospective clinical study.* Acta Neurochir (Wien), 2009. 151(5): p. 537-43.
175. Knopp, U., et al., *A new collagen biomatrix of equine origin versus a cadaveric dura graft for the repair of dural defects--a comparative animal experimental study.* Acta Neurochir (Wien), 2005. 147(8): p. 877-87.
176. Yu, F., et al., *Current developments in dural repair: a focused review on new methods and materials.* Front Biosci (Landmark Ed), 2013. 18: p. 1335-43.
177. Neulen, A., et al., *Evaluation of efficacy and biocompatibility of a novel semisynthetic collagen matrix as a dural onlay graft in a large animal model.* Acta Neurochir (Wien), 2011. 153(11): p. 2241-50.
178. Yamagata, S., et al., *Clinical experience with expanded polytetrafluoroethylene sheet used as an artificial dura mater.* Neurol Med Chir (Tokyo), 1993. 33(8): p. 582-5.
179. Boop, F.A. and W.M. Chadduck, *Silastic duraplasty in pediatric patients.* Neurosurgery, 1991. 29(5): p. 785-7; discussion 788.

180. Nunamaker, E.A., K.J. Otto, and D.R. Kipke, *Investigation of the material properties of alginate for the development of hydrogel repair of dura mater.* Journal of the Mechanical Behavior of Biomedical Materials, 2011. 4(1): p. 16-33.
181. Pogorielov, M., et al., *Experimental evaluation of new chitin-chitosan graft for duraplasty.* J Mater Sci Mater Med, 2017. 28(2): p. 34.
182. Luis Renato, M., et al., *Duraplasty with biosynthetic cellulose: an experimental study.* Journal of Neurosurgery, 1997. 86(1): p. 143-150.
183. Lima, F.d.M.T.d., et al., *Biocompatible bacterial cellulose membrane in dural defect repair of rat.* Journal of Materials Science: Materials in Medicine, 2017. 28(3): p. 37.
184. Narotam, P.K., et al., *Collagen matrix duraplasty for cranial and spinal surgery: a clinical and imaging study.* J Neurosurg, 2007. 106(1): p. 45-51.
185. Filippi, R., et al., *Bovine pericardium for duraplasty: Clinical results in 32 patients.* Neurosurgical review, 2001. 24: p. 103-7.
186. Narotam, P.K., F. Qiao, and N. Nathoo, *Collagen matrix duraplasty for posterior fossa surgery: evaluation of surgical technique in 52 adult patients. Clinical article.* J Neurosurg, 2009. 111(2): p. 380-6.
187. Lewis, K.M., et al., *Safety and Efficacy of a Novel, Self-Adhering Dural Substitute in a Canine Supratentorial Durotomy Model.* Neurosurgery, 2018. 82(3): p. 397-406.
188. Azzam, D., et al., *Dural Repair in Cranial Surgery Is Associated with Moderate Rates of Complications with Both Autologous and Nonautologous Dural Substitutes.* World Neurosurg, 2018. 113: p. 244-248.
189. Ahmed, E.M., *Hydrogel: Preparation, characterization, and applications: A review.* Journal of Advanced Research, 2015. 6(2): p. 105-121.
190. Kang, H.W., Y. Tabata, and Y. Ikada, *Fabrication of porous gelatin scaffolds for tissue engineering.* Biomaterials, 1999. 20(14): p. 1339-44.
191. Dinescu, S., et al., *Collagen-Based Hydrogels and Their Applications for Tissue Engineering and Regenerative Medicine*, in *Cellulose-Based Superabsorbent Hydrogels*, M.I.H. Mondal, Editor. 2019, Springer International Publishing: Cham. p. 1643-1664.
192. Chan, A.W., R.A. Whitney, and R.J. Neufeld, *Semisynthesis of a controlled stimuli-responsive alginate hydrogel.* Biomacromolecules, 2009. 10(3): p. 609-16.
193. Chang, C. and L. Zhang, *Cellulose-based hydrogels: Present status and application prospects.* Carbohydrate Polymers, 2011. 84(1): p. 40-53.
194. Nie, H., et al., *Factors on the preparation of carboxymethylcellulose hydrogel and its degradation behavior in soil.* Carbohydrate Polymers, 2004. 58(2): p. 185-189.
195. Lin, C.-C. and K.S. Anseth, *PEG Hydrogels for the Controlled Release of Biomolecules in Regenerative Medicine.* Pharmaceutical Research, 2009. 26(3): p. 631-643.
196. Jiang, S., S. Liu, and W. Feng, *PVA hydrogel properties for biomedical application.* Journal of the Mechanical Behavior of Biomedical Materials, 2011. 4(7): p. 1228-1233.
197. Bostan, L., et al., *Mechanical and tribological properties of poly(hydroxyethyl methacrylate) hydrogels as articular cartilage substitutes.* Tribology International, 2012. 46(1): p. 215-224.
198. Mantha, S., et al., *Smart Hydrogels in Tissue Engineering and Regenerative Medicine.* Materials (Basel), 2019. 12(20).
199. Zhu, J. and R.E. Marchant, *Design properties of hydrogel tissue-engineering scaffolds.* Expert Rev Med Devices, 2011. 8(5): p. 607-26.
200. Tan, H. and K.G. Marra, *Injectable, Biodegradable Hydrogels for Tissue Engineering Applications.* Materials, 2010. 3(3): p. 1746-1767.
201. Lee, K. and D. Mooney, *Hydrogels for Tissue Engineering.* Chemical reviews, 2001. 101: p. 1869-79.
202. Weinstein, J.S., et al., *The safety and effectiveness of a dural sealant system for use with nonautologous duraplasty materials.* Journal of neurosurgery, 2010. 112(2): p. 428-433.

203. *Synthetic Hydrogel Guidance Channels Facilitate Regeneration of Adult Rat Brainstem Motor Axons after Complete Spinal Cord Transection.* Journal of Neurotrauma, 2004. 21(6): p. 789-804.
204. Zhong, J., et al., *Hydrogel matrix to support stem cell survival after brain transplantation in stroke.* Neurorehabil Neural Repair, 2010. 24(7): p. 636-44.
205. Cook, D.J., et al., *Hydrogel-delivered brain-derived neurotrophic factor promotes tissue repair and recovery after stroke.* J Cereb Blood Flow Metab, 2017. 37(3): p. 1030-1045.
206. Gorenkova, N., et al., *In Vivo Evaluation of Engineered Self-Assembling Silk Fibroin Hydrogels after Intracerebral Injection in a Rat Stroke Model.* ACS Biomaterials Science & Engineering, 2018. 5.
207. Wang, Y., et al., *Hydrogel delivery of erythropoietin to the brain for endogenous stem cell stimulation after stroke injury.* Biomaterials, 2012. 33(9): p. 2681-92.
208. Xu, J., et al., *Injectable Gelatin Hydrogel Suppresses Inflammation and Enhances Functional Recovery in a Mouse Model of Intracerebral Hemorrhage.* Front Bioeng Biotechnol, 2020. 8: p. 785.
209. Ma, J., et al., *An experimental test of stroke recovery by implanting a hyaluronic acid hydrogel carrying a Nogo receptor antibody in a rat model.* Biomedical Materials, 2007. 2(4): p. 233.
210. Srivastava, L.M., *CHAPTER 2 - Cell Wall, Cell Division, and Cell Growth*, in *Plant Growth and Development*, L.M. Srivastava, Editor. 2002, Academic Press: San Diego. p. 23-74.
211. Nishiyama, Y., P. Langan, and H. Chanzy, *Crystal Structure and Hydrogen-Bonding System in Cellulose Iβ from Synchrotron X-ray and Neutron Fiber Diffraction.* Journal of the American Chemical Society, 2002. 124(31): p. 9074-9082.
212. George, J. and S. N, *Cellulose nanocrystals: Synthesis, functional properties, and applications.* Nanotechnology, Science and Applications, 2015. 8: p. 45.
213. Huang, Y., et al., *Recent advances in bacterial cellulose.* Cellulose, 2014. 21.
214. Azeredo, H.M.C., et al., *Bacterial Cellulose as a Raw Material for Food and Food Packaging Applications.* Frontiers in Sustainable Food Systems, 2019. 3(7).
215. Sukara, E., *Potential Values of Bacterial cellulose for industrial aPPlications.* Jurnal Selulosa, Vol. 4, No. 1, Juni 2014 : 7 - 16, 2014. Volume 4: p. 7-16.
216. Luo, M.T., et al., *Cellulose-Based Absorbent Production from Bacterial Cellulose and Acrylic Acid: Synthesis and Performance.* Polymers (Basel), 2018. 10(7).
217. Brigham, C., *Chapter 3.22 - Biopolymers: Biodegradable Alternatives to Traditional Plastics*, in *Green Chemistry*, B. Török and T. Dransfield, Editors. 2018, Elsevier. p. 753-770.
218. Klemm, D., et al., *Cellulose: fascinating biopolymer and sustainable raw material.* Angew Chem Int Ed Engl, 2005. 44(22): p. 3358-93.
219. Stumpf, T.R., et al., *In situ and ex situ modifications of bacterial cellulose for applications in tissue engineering.* Materials Science and Engineering: C, 2018. 82: p. 372-383.
220. Recouvreux, D.O.S., et al., *Novel three-dimensional cocoon-like hydrogels for soft tissue regeneration.* Materials Science and Engineering C, Biomimetic Materials, Sensors and Systems, 2011. 31(2): p. 151-157.
221. Sokolnicki, A.M., et al., *Permeability of bacterial cellulose membranes.* Journal of Membrane Science, 2006. 272(1): p. 15-27.
222. Barud, H.S., et al., *Bacterial cellulose/poly(3-hydroxybutyrate) composite membranes.* Carbohydrate Polymers, 2011. 83(3): p. 1279-1284.
223. Baumgartner, S., J. Kristl, and N.A. Peppas, *Network structure of cellulose ethers used in pharmaceutical applications during swelling and at equilibrium.* Pharm Res, 2002. 19(8): p. 1084-90.
224. Peppas, N.A., *Hydrogels and drug delivery.* Current Opinion in Colloid & Interface Science, 1997. 2(5): p. 531-537.
225. Drury, J.L. and D.J. Mooney, *Hydrogels for tissue engineering: scaffold design variables and applications.* Biomaterials, 2003. 24(24): p. 4337-4351.

226. Stabenfeldt, S., A. García, and M. Laplaca, *Thermoreversible laminin-functionalized hydrogel for neural tissue engineering.* Journal of biomedical materials research. Part A, 2006. 77: p. 718-25.
227. Fellah, B., et al., *Bone repair using a new injectable self-crosslinkable bone substitute.* Journal of orthopaedic research : official publication of the Orthopaedic Research Society, 2006. 24: p. 628-35.
228. Czaja, W.K., et al., *The future prospects of microbial cellulose in biomedical applications.* Biomacromolecules, 2007. 8(1): p. 1-12.
229. Sannino, A., et al., *Crosslinking of cellulose derivatives and hyaluronic acid with water-soluble carbodiimide.* Polymer, 2005. 46(25): p. 11206-11212.
230. Xu, C., et al., *Bacterial cellulose membranes used as artificial substitutes for dural defection in rabbits.* Int J Mol Sci, 2014. 15(6): p. 10855-67.
231. Xu, C., et al., *Sustained release of vancomycin from bacterial cellulose membrane as dural substitutes for anti-inflammatory wound closure in rabbits.* Journal of Biomaterials Applications, 2020. 34(10): p. 1470-1478.
232. Rosen, C., et al., *Results of the Prospective, Randomized, Multicenter Clinical Trial Evaluating a Biosynthesized Cellulose Graft for Repair of Dural Defects.* Neurosurgery, 2011. 69: p. 1093 1104.
233. Li, J. and D.J. Mooney, *Designing hydrogels for controlled drug delivery.* Nature reviews. Materials, 2016. 1(12): p. 16071.
234. Sanadgol, N. and J. Wackerlig, *Developments of Smart Drug-Delivery Systems Based on Magnetic Molecularly Imprinted Polymers for Targeted Cancer Therapy: A Short Review.* Pharmaceutics, 2020. 12(9).
235. Rosina, A., A. Mathew, and O. Mohammed, *CONVENTIONAL Vs CONTROLLED DRUG DELIVERY SYSTEMS*. 2018.
236. *6 - Drug delivery systems*, in *Strategies to Modify the Drug Release from Pharmaceutical Systems*, M.L. Bruschi, Editor. 2015, Woodhead Publishing. p. 87-194.
237. Liestyo, l., et al., *Drug delivery systems improve Pharmaceutical profile and facilitate medication adherence.* Advances in therapy, 2005. 22: p. 559-77.
238. Bhowmik, D., et al., *Controlled Release Drug Delivery Systems.* The Pharma Innovation Journal, 2012. 1: p. 24-32.
239. Stevanović, M. and D. Uskokovi, *Poly(lactide-co-glycolide)-based Micro and Nanoparticles for the Controlled Drug Delivery of Vitamins.* Current Nanoscience - CURR NANOSCI, 2009. 5.
240. Priya James, H., et al., *Smart polymers for the controlled delivery of drugs – a concise overview.* Acta Pharmaceutica Sinica B, 2014. 4(2): p. 120-127.
241. Song, R., et al., *Current development of biodegradable polymeric materials for biomedical applications.* Drug Des Devel Ther, 2018. 12: p. 3117-3145.
242. Kiradzhiyska, D. and R. Mantcheva, *Overview of Biocompatible Materials and Their Use in Medicine.* Folia Medica, 2019. 61: p. 34-40.
243. Liechty, W.B., et al., *Polymers for drug delivery systems.* Annual review of chemical and biomolecular engineering, 2010. 1: p. 149-173.
244. Stewart, S.A., et al., *Implantable Polymeric Drug Delivery Devices: Classification, Manufacture, Materials, and Clinical Applications.* Polymers, 2018. 10(12): p. 1379.
245. Song, R., et al., *Current development of biodegradable polymeric materials for biomedical applications.* Drug design, development and therapy, 2018. 12: p. 3117-3145.
246. Nair, L. and C. Laurencin, *Polymers as Biomaterials for Tissue Engineering and Controlled Drug Delivery.* Advances in biochemical engineering/biotechnology, 2006. 102: p. 47-90.
247. Bhat, S. and A. Kumar, *Biomaterials in Regenerative Medicine.* Journal of Postgraduate Medicine Education and Research, 2012. 46: p. 81-89.
248. Dhandayuthapani, B., et al., *Polymeric Scaffolds in Tissue Engineering Application: A Review.* International Journal of Polymer Science, 2011. 2011: p. 290602.
249. Ulery, B.D., L.S. Nair, and C.T. Laurencin, *Biomedical Applications of Biodegradable Polymers.* Journal of polymer science. Part B, Polymer physics, 2011. 49(12): p. 832-864.

250. Soppimath, K., et al., *Biodegradable Polymeric Nanoparticles as Drug Delivery Devices.* Journal of Controlled Release, 2001. 70: p. 1-20.
251. Sung, Y.K. and S.W. Kim, *Recent advances in polymeric drug delivery systems.* Biomater Res, 2020. 24: p. 12.
252. Commandeur, S., H.M. van Beusekom, and W.J. van der Giessen, *Polymers, drug release, and drug-eluting stents.* J Interv Cardiol, 2006. 19(6): p. 500-6.
253. *Controlled Release Technology*, in *Encyclopedia of Polymer Science and Technology*.
254. Yang, W.-W. and E. Pierstorff, *Reservoir-Based Polymer Drug Delivery Systems*. Journal of Laboratory Automation, 2012. 17(1): p. 50-58.
255. Cauchetier, E., et al., *Atovaquone-loaded nanocapsules: influence of the nature of the polymer on their in vitro characteristics.* Int J Pharm, 2003. 250(1): p. 273-81.
256. Langer, R., *New methods of drug delivery.* Science, 1990. 249(4976): p. 1527-33.
257. Freiberg, S. and X. Zhu, *Polymer microspheres for controlled drug release.* International Journal of Pharmaceutics, 2004. 282: p. 1-18.
258. Lee, J.H. and Y. Yeo, *Controlled Drug Release from Pharmaceutical Nanocarriers*. Chemical engineering science, 2015. 125: p. 75-84.
259. Nish, S., G. Mathew, and J. Lincy, *Matrix Tablets: An Effective Way for Oral Controlled Release Drug Delivery.* Iranian Journal of Pharmaceutical Sciences, 2012. 8(3): p. 165-170.
260. Keraliya, R.A., et al., *Osmotic drug delivery system as a part of modified release dosage form.* ISRN pharmaceutics, 2012. 2012: p. 528079-528079.
261. Herrlich, S., et al., *Osmotic micropumps for drug delivery.* Adv Drug Deliv Rev, 2012. 64(14): p. 1617-27.
262. Ghosh, T. and A. Ghosh, *Drug delivery through osmotic systems - An overview*. Journal of Applied Pharmaceutical Science, 2011. 1: p. 38-49.
263. Sahoo, C.K., et al., *A review on controlled porosity osmotic pump tablets and its evaluation.* Bulletin of Faculty of Pharmacy, Cairo University, 2015. 53(2): p. 195-205.
264. *Nidhi Patel et al, Controlled Drug Delivery System: A Review, Indo Am. J. Pharm. Sci, 2016; 3(3).*
265. Peppas, N.A., et al., *Hydrogels in pharmaceutical formulations*. Eur J Pharm Biopharm, 2000. 50(1): p. 27-46.
266. Lin, C.C. and A.T. Metters, *Hydrogels in controlled release formulations: network design and mathematical modeling.* Adv Drug Deliv Rev, 2006. 58(12-13): p. 1379-408.
267. Lee, P.I., *Novel approach to zero-order drug delivery via immobilized nonuniform drug distribution in glassy hydrogels*. J Pharm Sci, 1984. 73(10): p. 1344-7.
268. Kaity, S., J. Isaac, and A. Ghosh, *Interpenetrating polymer network of locust bean gum-poly (vinyl alcohol) for controlled release drug delivery.* Carbohydr Polym, 2013. 94(1): p. 456-67.
269. *4 - Main mechanisms to control the drug release*, in *Strategies to Modify the Drug Release from Pharmaceutical Systems*, M.L. Bruschi, Editor. 2015, Woodhead Publishing. p. 37-62.
270. Kamaly, N., et al., *Degradable Controlled-Release Polymers and Polymeric Nanoparticles: Mechanisms of Controlling Drug Release.* Chem Rev, 2016. 116(4): p. 2602-63.
271. von Burkersroda, F., L. Schedl, and A. Göpferich, *Why degradable polymers undergo surface erosion or bulk erosion.* Biomaterials, 2002. 23(21): p. 4221-31.
272. Fredenberg, S., et al., *The mechanisms of drug release in poly(lactic-co-glycolic acid)-based drug delivery systems--a review.* Int J Pharm, 2011. 415(1-2): p. 34-52.
273. Wadhwa, S. and R.J. Mumper, *Polymer-Drug Conjugates for Anticancer Drug Delivery.* Crit Rev Ther Drug Carrier Syst, 2015. 32(3): p. 215-45.
274. Macdougall, L., et al., *1.3.2F - Degradable and Resorbable Polymers*, in *Biomaterials Science (Fourth Edition)*, W.R. Wagner, et al., Editors. 2020, Academic Press. p. 167-190.
275. Fu, Y. and W.J. Kao, *Drug release kinetics and transport mechanisms of non-degradable and degradable polymeric delivery systems*. Expert opinion on drug delivery, 2010. 7(4): p. 429-444.

276. Raval, A., J. Parikh, and C. Engineer, *Mechanism of controlled release kinetics from medical devices.* Brazilian Journal of Chemical Engineering, 2010. 27: p. 211-225.
277. Ribeiro, L.N.M., et al., *Advances in Hybrid Polymer-Based Materials for Sustained Drug Release.* International Journal of Polymer Science, 2017. 2017: p. 1-16.
278. Gavasane, A. and H. Pawar, *Synthetic Biodegradable Polymers Used in Controlled Drug Delivery System: An Overview.* Clinical Pharmacology & Biopharmaceutics, 2014. 3: p. 121.
279. Ghasemiyeh, P. and S. Mohammadi Samani, *Hydrogels as Drug Delivery Systems; Pros and Cons (Review Article).* 2019. 5: p. 7-24.
280. Al Malyan, M., et al., *Polymer-Based Biodegradable Drug Delivery Systems in Pain Management.* The Journal of craniofacial surgery, 2006. 17: p. 302-13.
281. Sercombe, L., et al., *Advances and Challenges of Liposome Assisted Drug Delivery.* Frontiers in pharmacology, 2015. 6: p. 286-286.
282. Kim, K.K. and D.W. Pack, *Microspheres for Drug Delivery*, in *BioMEMS and Biomedical Nanotechnology: Volume I Biological and Biomedical Nanotechnology*, M. Ferrari, A.P. Lee, and L.J. Lee, Editors. 2006, Springer US: Boston, MA. p. 19-50.
283. K.H, R., *Microspheres: as carrieres used for novel drug delivery system.* IOSR Journal of Pharmacy (IOSRPHR), 2012. 2: p. 44-48.
284. Hossain, K.M.Z., U. Patel, and I. Ahmed, *Development of microspheres for biomedical applications: a review.* Prog Biomater, 2015. 4(1): p. 1-19.
285. Bhatia, S., *Natural Polymers vs Synthetic Polymer*. 2016. p. 95-118.
286. Vroman, I. and L. Tighzert, *Biodegradable Polymers.* Materials, 2009. 2(2): p. 307-344.
287. Simionescu, B.C. and D. Ivanov, *Natural and Synthetic Polymers for Designing Composite Materials*, in *Handbook of Bioceramics and Biocomposites*, I.V. Antoniac, Editor. 2016, Springer International Publishing: Cham. p. 233-286.
288. Doppalapudi, S., et al., *Biodegradable Natural Polymers*, in *Advanced Polymers in Medicine*, F. Puoci, Editor. 2015, Springer International Publishing: Cham. p. 33-66.
289. Liu, S., et al., *Current applications of poly(lactic acid) composites in tissue engineering and drug delivery.* Composites Part B: Engineering, 2020. 199: p. 108238.
290. Makadia, H.K. and S.J. Siegel, *Poly Lactic-co-Glycolic Acid (PLGA) as Biodegradable Controlled Drug Delivery Carrier.* Polymers (Basel), 2011. 3(3): p. 1377-1397.
291. Stratton, S., et al., *Bioactive polymeric scaffolds for tissue engineering.* Bioactive Materials, 2016. 1(2): p. 93-108.
292. Elmowafy, E., M. Tiboni, and M. Soliman, *Biocompatibility, biodegradation and biomedical applications of poly(lactic acid)/poly(lactic-co-glycolic acid) micro and nanoparticles.* Journal of Pharmaceutical Investigation, 2019. 49.
293. Qi, F., et al., *Recent research and development of PLGA/PLA microspheres/nanoparticles: A review in scientific and industrial aspects.* Frontiers of Chemical Science and Engineering, 2019. 13(1): p. 14-27.
294. Blasi, P., *Poly(lactic acid)/poly(lactic-co-glycolic acid)-based microparticles: an overview.* Journal of Pharmaceutical Investigation, 2019. 49(4): p. 337-346.
295. Ko, J.T., et al., *The Double-Layered Microsphere: Encapsulation of Water-Soluble Protein with PLGA.* Key Engineering Materials, 2007. 342-343: p. 513-516.
296. Hyon, S.H., *Biodegradable poly (lactic acid) microspheres for drug delivery systems.* Yonsei Med J, 2000. 41(6): p. 720-34.
297. Alexis, F., *Factors affecting the degradation and drug-release mechanism of poly(lactic acid) and poly[(lactic acid)-co-(glycolic acid)].* Polymer International, 2005. 54: p. 36-46.
298. Arpagaus, C., *PLA/PLGA nanoparticles prepared by nano spray drying.* Journal of Pharmaceutical Investigation, 2019. 49(4): p. 405-426.
299. *Fabrication and Characterization of PLA-PGA Orthopedic Implants.* Tissue Engineering, 1995. 1(3): p. 241-252.

300. Lagreca, E., et al., *Recent advances in the formulation of PLGA microparticles for controlled drug delivery.* Progress in Biomaterials, 2020. 9(4): p. 153-174.
301. *Wikimedia Commons, "Polylactid sceletal," [Online].* . Available from: https://commons.wikimedia.org/w/index.php?curid=4227746.
302. Huang, X. and C.S. Brazel, *On the importance and mechanisms of burst release in matrix-controlled drug delivery systems.* Journal of Controlled Release, 2001. 73(2): p. 121-136.
303. Rahman, N.A. and E. Mathiowitz, *Localization of bovine serum albumin in double-walled microspheres.* J Control Release, 2004. 94(1): p. 163-75.
304. Zheng, W., *A water-in-oil-in-oil-in-water (W/O/O/W) method for producing drug-releasing, double-walled microspheres.* Int J Pharm, 2009. 374(1-2): p. 90-5.
305. Ansary, R.H., et al., *Controlled Release of Lysozyme from Double-Walled Poly(Lactide-Co-Glycolide) (PLGA) Microspheres.* Polymers (Basel), 2017. 9(10).
306. Xu, Q., et al., *Mechanism of drug release from double-walled PDLLA(PLGA) microspheres.* Biomaterials, 2013. 34(15): p. 3902-11.
307. Ansary, R.H., et al., *Preparation, characterization and in vitro release study of BSA-loaded double-walled glucose-poly(lactide-co-glycolide) microspheres.* Arch Pharm Res, 2016. 39(9): p. 1242-56.
308. Lee, T.H., J. Wang, and C.H. Wang, *Double-walled microspheres for the sustained release of a highly water soluble drug: characterization and irradiation studies.* J Control Release, 2002. 83(3): p. 437-52.
309. Navaei, A., et al., *Double-walled microspheres loaded with meglumine antimoniate: preparation, characterization and in vitro release study.* Drug Dev Ind Pharm, 2014. 40(6): p. 701-10.
310. Freitas, S., H.P. Merkle, and B. Gander, *Microencapsulation by solvent extraction/evaporation: reviewing the state of the art of microsphere preparation process technology.* J Control Release, 2005. 102(2): p. 313-32.
311. Deshmukh, R., P. Wagh, and J. Naik, *Solvent evaporation and spray drying technique for micro- and nanospheres/particles preparation: A review.* Drying Technology, 2016. 34(15): p. 1758-1772.
312. Xu, Y., et al., *Optimization of electrospray fabrication of stem cell–embedded alginate–gelatin microspheres and their assembly in 3D-printed poly(ε-caprolactone) scaffold for cartilage tissue engineering.* Journal of Orthopaedic Translation, 2019. 18: p. 128-141.
313. Liu, F., et al., *Preparation of chitosan–hyaluronate double-walled microspheres by emulsification-coacervation method.* Journal of Materials Science: Materials in Medicine, 2007. 18(11): p. 2215-2224.
314. Ciombor, D.M., et al., *Encapsulation of BSA using a modified W/O/O emulsion solvent removal method.* J Microencapsul, 2006. 23(2): p. 183-94.
315. Kim, B.S., et al., *BSA-FITC-loaded microcapsules for in vivo delivery.* Biomaterials, 2009. 30(5): p. 902-9.
316. Xiao, C.D., X.C. Shen, and L. Tao, *Modified emulsion solvent evaporation method for fabricating core-shell microspheres.* Int J Pharm, 2013. 452(1-2): p. 227-32.
317. Lee, W.L. and S.C. Loo, *Revolutionizing drug delivery through biodegradable multilayered particles.* J Drug Target, 2012. 20(8): p. 633-47.
318. Pekarek, K.J., J.S. Jacob, and E. Mathiowltz, *Double-Walled Microspheres for Drug Delivery.* MRS Proceedings, 2011. 331: p. 97.
319. Pollauf, E.J. and D.W. Pack, *Use of thermodynamic parameters for design of double-walled microsphere fabrication methods.* Biomaterials, 2006. 27(14): p. 2898-2906.
320. Pekarek, K.J., J.S. Jacob, and E. Mathiowitz, *Double-walled polymer microspheres for controlled drug release.* Nature, 1994. 367(6460): p. 258-60.
321. Pekarek, K.J., J.S. Jacob, and E. Mathiowitz, *One-step preparation of double-walled microspheres.* Advanced Materials, 1994. 6(9): p. 684-687.

322. Lee, W.L., E. Widjaja, and S.C.J. Loo, *Designing drug-loaded multi-layered polymeric microparticles.* Journal of Materials Science: Materials in Medicine, 2012. 23(1): p. 81-88.
323. Caicco, M.J., et al., *A hydrogel composite system for sustained epi-cortical delivery of Cyclosporin A to the brain for treatment of stroke.* J Control Release, 2013. 166(3): p. 197-202.
324. Ju, R., et al., *The experimental therapy on brain ischemia by improvement of local angiogenesis with tissue engineering in the mouse.* Cell Transplant, 2014. 23 Suppl 1: p. S83-95.
325. Bertram, J.P., et al., *Using polymer chemistry to modulate the delivery of neurotrophic factors from degradable microspheres: delivery of BDNF.* Pharm Res, 2010. 27(1): p. 82-91.
326. Jin, Y., et al., *Biodegradable gelatin microspheres enhance the neuroprotective potency of osteopontin via quick and sustained release in the post-ischemic brain.* Acta Biomater, 2014. 10(7): p. 3126-35.
327. Ali, Z., et al., *Adjustable delivery of pro-angiogenic FGF-2 by alginate:collagen microspheres.* Biol Open, 2018. 7(3).
328. Klose, D., et al., *Fenofibrate-loaded PLGA microparticles: effects on ischemic stroke.* European journal of pharmaceutical sciences : official journal of the European Federation for Pharmaceutical Sciences, 2009. 37(1): p. 43-52.
329. Hazekawa, M., et al., *Single injection of ONO-1301-loaded PLGA microspheres directly after ischaemia reduces ischaemic damage in rats subjected to middle cerebral artery occlusion.* J Pharm Pharmacol, 2012. 64(3): p. 353-9.
330. Nakaguchi, K., et al., *Growth factors released from gelatin hydrogel microspheres increase new neurons in the adult mouse brain.* Stem Cells Int, 2012. 2012: p. 915160.
331. Bible, E., et al., *The support of neural stem cells transplanted into stroke-induced brain cavities by PLGA particles.* Biomaterials, 2009. 30(16): p. 2985-94.
332. Memanishvili, T., et al., *Poly(ester amide) microspheres are efficient vehicles for long-term intracerebral growth factor delivery and improve functional recovery after stroke.* Biomed Mater, 2020. 15(6): p. 065020.
333. *Combined Transplantation of Bone Marrow Stromal Cell-Derived Neural Progenitor Cells with a Collagen Sponge and Basic Fibroblast Growth Factor Releasing Microspheres Enhances Recovery After Cerebral Ischemia in Rats.* Tissue Engineering Part A, 2011. 17(15-16): p. 1993-2004.
334. Jin, Y.C., et al., *The effect of biodegradable gelatin microspheres on the neuroprotective effects of high mobility group box 1 A box in the postischemic brain.* Biomaterials, 2011. 32(3): p. 899-908.
335. Lee, T., J. Wang, and C.-H. Wang, *Double-walled microspheres for the sustained release of a highly water soluble drug: Characterization and irradiation studies.* Journal of controlled release : official journal of the Controlled Release Society, 2002. 83: p. 437-52.
336. Cao, X. and M.S. Schoichet, *Delivering neuroactive molecules from biodegradable microspheres for application in central nervous system disorders.* Biomaterials, 1999. 20(4): p. 329-39.
337. Leach, K., K. Noh, and E. Mathiowitz, *Effect of manufacturing conditions on the formation of double-walled polymer microspheres.* J Microencapsul, 1999. 16(2): p. 153-67.
338. Hong, Y., et al., *Preparation of porous polylactide microspheres by emulsion-solvent evaporation based on solution induced phase separation.* Polymers for Advanced Technologies, 2005. 16: p. 622-627.
339. Subedi, G., A. Shrestha, and S. Shakya. *Study of Effect of Different Factors in Formulation of Micro and Nanospheres with Solvent Evaporation Technique*. 2016.
340. Mufassir Mushtaque, M., et al., *Effects of solvents: preparation and characterization of sustained release intranasal microspheres of rizatriptan benzoate.* Journal of Innovations in Pharmaceuticals and Biological Science, 2014. 1: p. 68-79.
341. Rahman, H., C. Thomas, and K. Kuppusamy, *Comparative evaluation of HPMC K100 and poloxamer 188-influence on release kinetics of curcumin in floating microspheres.* Research Journal of Pharmaceutical, Biological and Chemical Sciences, 2010. 1: p. 28-34.

342. Dorati, R., et al., *An experimental design approach to the preparation of pegylated polylactide-co-glicolide gentamicin loaded microparticles for local antibiotic delivery.* Materials Science and Engineering: C, 2016. 58: p. 909-917.
343. Kokai, L.E., A.M. Ghaznavi, and K.G. Marra, *Incorporation of double-walled microspheres into polymer nerve guides for the sustained delivery of glial cell line-derived neurotrophic factor.* Biomaterials, 2010. 31(8): p. 2313-22.
344. Dutta, D., et al., *Tunable delayed controlled release profile from layered polymeric microparticles.* J Mater Chem B, 2017. 5(23): p. 4487-4498.
345. Zhao, H., J. Gagnon, and U.O. Häfeli, *Process and formulation variables in the preparation of injectable and biodegradable magnetic microspheres.* Biomagnetic research and technology, 2007. 5: p. 2-2.
346. Ghaderi, R. and J. Carlfors, *Biological activity of lysozyme after entrapment in poly(d,l-lactide-co-glycolide)-microspheres.* Pharm Res, 1997. 14(11): p. 1556-62.
347. Srivastava, A., D. Ridhurkar, and S. Wadhwa, *Floating microspheres of Cimetidine: Formulation, characterization and in vitro evaluation.* Acta pharmaceutica (Zagreb, Croatia), 2005. 55: p. 277-85.
348. Thanh Ha, H., et al., *Cross-flow membrane emulsification technique for fabrication of drug-loaded particles.* Advances in Natural Sciences: Nanoscience and Nanotechnology, 2013. 4: p. 045008.
349. Ahangaran, F., A.H. Navarchian, and F. Picchioni, *Material encapsulation in poly(methyl methacrylate) shell: A review.* Journal of Applied Polymer Science, 2019. 136(41): p. 48039.
350. Yang, Y.Y., T.S. Chung, and N.P. Ng, *Morphology, drug distribution, and in vitro release profiles of biodegradable polymeric microspheres containing protein fabricated by double-emulsion solvent extraction/evaporation method.* Biomaterials, 2001. 22(3): p. 231-41.
351. Dinarvand, R., et al., *Preparation of biodegradable microspheres and matrix devices containing naltrexone.* AAPS PharmSciTech, 2003. 4(3): p. 45-54.
352. Matsumoto, A., et al., *The polymer-alloys method as a new preparation method of biodegradable microspheres: principle and application to cisplatin-loaded microspheres.* Journal of Controlled Release, 1997. 48(1): p. 19-27.
353. Bodmeier, R. and J.W. McGinity, *Solvent selection in the preparation of poly(dl-lactide) microspheres prepared by the solvent evaporation method.* International Journal of Pharmaceutics, 1988. 43(1): p. 179-186.
354. Maa, Y.F. and C.C. Hsu, *Effect of primary emulsions on microsphere size and protein-loading in the double emulsion process.* J Microencapsul, 1997. 14(2): p. 225-41.
355. Crotts, G. and T.G. Park, *Preparation of porous and nonporous biodegradable polymeric hollow microspheres.* Journal of Controlled Release, 1995. 35(2): p. 91-105.
356. Zhang, G., et al., *Fabrication of hollow porous PLGA microspheres for controlled protein release and promotion of cell compatibility.* Chinese Chemical Letters, 2013. 24: p. 710-714.
357. Shi, M., et al., *Double walled POE/PLGA microspheres: encapsulation of water-soluble and water-insoluble proteins and their release properties.* Journal of Controlled Release, 2003. 89(2): p. 167-177.
358. Godbee, J., P. Weston, and E. Mathiowitz, *The effects of infiltration on protein release from multi-phase microspheres fabricated via solvent removal.* J Microencapsul, 2002. 19(6): p. 783-96.
359. *5 - Mathematical models of drug release*, in *Strategies to Modify the Drug Release from Pharmaceutical Systems*, M.L. Bruschi, Editor. 2015, Woodhead Publishing. p. 63-86.
360. Mircioiu, C., et al., *Mathematical Modeling of Release Kinetics from Supramolecular Drug Delivery Systems.* Pharmaceutics, 2019. 11(3).
361. Dash, S., et al., *Kinetic modeling on drug release from controlled drug delivery systems.* Acta Pol Pharm, 2010. 67(3): p. 217-23.

362. Mulye, N. and S. Turco, *A Simple Model Based on First Order Kinetics to Explain Release of Highly Water Soluble Drugs from Porous Dicalcium Phosphate Dihydrate Matrices.* Drug Development and Industrial Pharmacy, 2008. 21: p. 943-953.
363. Higuchi, T., *MECHANISM OF SUSTAINED-ACTION MEDICATION. THEORETICAL ANALYSIS OF RATE OF RELEASE OF SOLID DRUGS DISPERSED IN SOLID MATRICES.* J Pharm Sci, 1963. 52: p. 1145-9.
364. Cheng, X., R. Liu, and Y. He, *A simple method for the preparation of monodisperse protein-loaded microspheres with high encapsulation efficiencies.* Eur J Pharm Biopharm, 2010. 76(3): p. 336-41.
365. Ferrero, C., D. Massuelle, and E. Doelker, *Towards elucidation of the drug release mechanism from compressed hydrophilic matrices made of cellulose ethers. II. Evaluation of a possible swelling-controlled drug release mechanism using dimensionless analysis.* J Control Release, 2010. 141(2): p. 223-33.
366. Hickey, T., et al., *Dexamethasone/PLGA microspheres for continuous delivery of an anti-inflammatory drug for implantable medical devices.* Biomaterials, 2002. 23(7): p. 1649-56.
367. Song, X., et al., *β-methasone-containing biodegradable poly(lactide-co-glycolide) acid microspheres for intraarticular injection: effect of formulation parameters on characteristics and in vitro release.* Pharm Dev Technol, 2013. 18(5): p. 1220-9.
368. Korsmeyer, R.W., et al., *Mechanisms of solute release from porous hydrophilic polymers.* International Journal of Pharmaceutics, 1983. 15(1): p. 25-35.
369. Lee, W.L., et al., *Fabrication and Drug Release Study of Double-Layered Microparticles of Various Sizes.* Journal of pharmaceutical sciences, 2012. 101: p. 2787-97.
370. Mainardes, R.M. and R.C. Evangelista, *PLGA nanoparticles containing praziquantel: effect of formulation variables on size distribution.* Int J Pharm, 2005. 290(1-2): p. 137-44.

7. Appendices

Appendix 1: DSC thermograms of the DWMS. (A) BSA solution loaded DWMS (1:1, w/w). (B) BSA powder loaded DWMS (1:1, w/w). (C) PLGA SWMS. (D) PLLA SWMS. (E) Blank DWMS (1:1, w/w).